in each well was determined at 490 nm using a microplate reader (Bio-Rad).

2.7. Viral antigen ELISA

HUT-102 cells (1×10^6) were cultured with 20 or 40 μg/ml DHMEQ for 16 h. Cell culture media were centrifuged at $1200 \times g$ for 10 min at 4 °C. HTLV-I p19 antigen was determined by ELISA according to the manufacturer's protocol (Zeptometrix, Buffalo, NY).

2.8. Hoechst 33342 stain

HUT-102 cells (1×10^6) in a 35-mm dish were cultured with 20 or 40 μg/ml DHMEQ for 48 h. Cells treated with DMSO solution lacking DHMEQ served as a control. Cells were then fixed with 1% glutaraldehyde for 30 min at room temperature and washed three times with PBS. Subsequently, they were stained with 5 μg/ml Hoechst 33342 (Calbiochem, San Diego, CA) for 5 min at room temperature and then washed three times with PBS. Stained apoptotic and non-apoptotic nuclei were photographed under UV light by a digital CCD camera (DP70; Olympus, Tokyo, Japan), and a total of 1000 cells were counted. MOLT-4 cells served as a control, using the same procedure.

2.9. Mice

SCID (C.B17-scid/scid) female mice, 4 weeks of age, were obtained from Charles River Japan, Inc. (Tokyo, Japan). The mice were maintained under specific pathogen-free conditions in laminar-flow benches at 22 ± 2 °C with a 12-h light/12-h dark cycle. Mice were fed sterilized (γ-irradiated) pellets and received hyperchlorinated water ad libitum. All procedures involving animals and their care were approved by the animal care committee of Kumamoto University in accordance with Institutional and Japanese government guidelines for animal experiments.

2.10. Inoculation of cells into SCID mice

HUT-102 cells were washed three times with PBS and resuspended in PBS. Five-week-old SCID mice were pretreated intraperitoneally with anti-murine interleukin-2 receptor (IL2R; 1 mg/mouse) β chain monoclonal antibody (mAb), TM-β1 [14], 3 days earlier to eliminate NK cell activity. Mice were anesthetized with ether, and the cells (5×10^7 per mouse) were inoculated subcutaneously in the postauricular region.

2.11. Administration of DHMEQ to SCID mice injected with HUT-102 cells

DHMEQ was dissolved in 0.5% carboxymethyl cellulose to a final concentration of 1.2 mg/ml. DHMEQ (12 mg/kg) or vehicle alone was administered to mice intraperitoneally or directly into the cell injection site subcutaneously on day 0 of cell inoculation and once daily thereafter until day 28. Both tumor size and body weight were measured daily. Tumor volume was calculated according to the formula: $a^2 \times b \times 0.5$, where a and b are the smallest and largest diameters, respectively. To examine whether inoculated cells translocated to other sites or formed tumors in mice, the mice were monitored using an X-ray computed tomography (CT) scanner (LaTheta; Aloka Co. Ltd., Tokyo, Japan).

2.12. Histology

Animals were sacrificed at day 30. Organs were fixed in 10% neutral-buffered formalin immediately after removal, embedded in paraffin, cut into 4-μm sections, and stained with hematoxylin and eosin (HE).

2.13. PCR

To detect HTLV-I genomic sequences, 0.5 μg DNA from tumors or various organs was subjected to PCR analysis as described previously [15,16], using oligonucleotide primers specific for *tax* or human *β-globin* genes.

2.14. Western blot analysis

A total of 50 μg of total protein lysate from tumors was electrophoresed and transferred to a polyvinylidene difluoride membrane (Atto, Tokyo, Japan). The filter was incubated with an anti-Tax mouse monoclonal antibody. The anti-Tax/HTLV-I Tax hybridoma 168A51-42 (Tab176) was obtained from Dr. Beatrice C. Langton through the AIDS Research and Reference Reagent Program, Division of AIDS, NIAID, NIH (Bethesda, MD). The membrane was then incubated with peroxidase-conjugated anti-mouse IgG (Cappel, Durham, NC) and then incubated with chemiluminescence reagents (ECL Plus; Amersham Pharmacia Biotech, Buckinghamshire, UK) and exposed to autoradiography film.

2.15. Statistical analysis

Statistical analysis was performed using the Student's t-test. Differences in data were considered statistically significant at $P < 0.05$.

3. Results

3.1. DHMEQ inhibits NF-κB in HUT-102 cells

We analyzed the HTLV-I-infected T-cell line, HUT-102, and uninfected T-cell line, MOLT-4, for NF-κB activation using ELISA. HUT-102 cells showed constitutive activation of NF-κB, which was elevated compared with MOLT-4 cells (Fig. 1A). We next examined the effects of DHMEQ on the constitutively active NF-κB in HUT-102 cells. The cells were
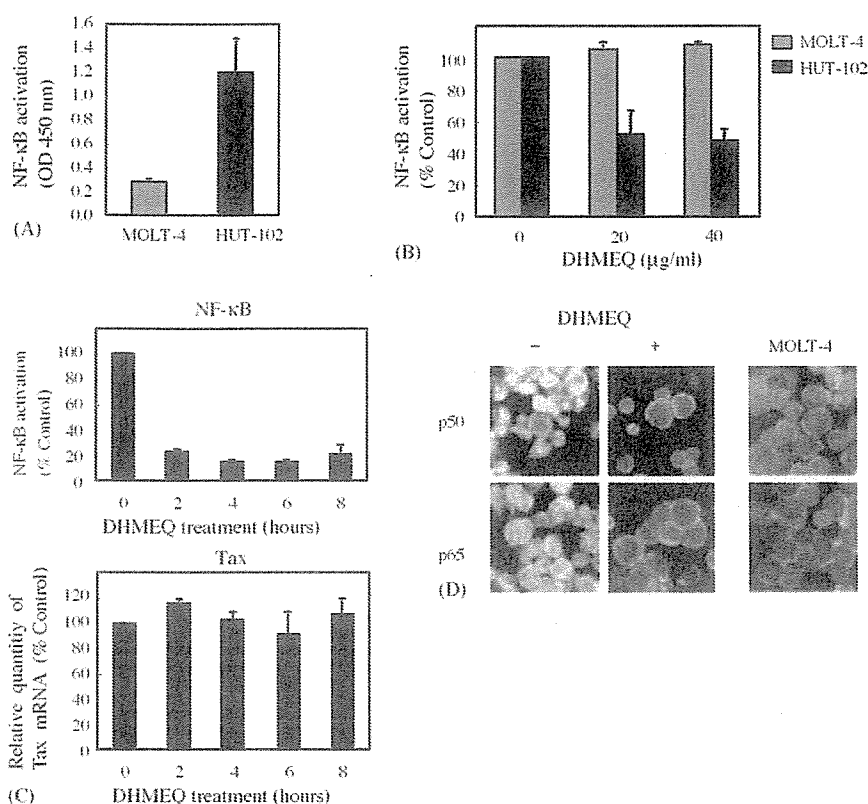
Fig. 1. DHMEQ inhibits NF-κB activity in HUT-102 cells. (A) NF-κB activity in the HTLV-I-infected T-cell line. HUT-102. and uninfected cell line. MOLT-4, was measured by ELISA. This experiment was repeated three times. and the data presented represent the mean ± standard deviation. (B) DHMEQ inhibits NF-κB activity. After a 16-h incubation. NF-κB activity was measured in cells treated with DHMEQ using ELISA. Data are expressed as a percentage of control (vehicle-treated) and represent the mean ± standard deviation. MOLT-4 cells served as the control. (C) The effect of DHMEQ on the expression of *tax*. HUT-102 cells were treated with 20 μg/ml DHMEQ and incubated for various periods. NF-κB activity in cells treated with DHMEQ was measured by ELISA (upper panel), and relative expression of *tax* was assessed by real-time RT-PCR (lower panel). Data are expressed as a percentage of the zero time point and represent the mean ± standard deviation. (D) Inhibition of nuclear translocation of NF-κB by DHMEQ. Representative results of immunofluorescence analyses in HUT-102 cells treated with DHMEQ for 16 h using antibodies against NF-κB p50 or p65. MOLT-4 cells served as the control.

cultured with various concentrations (0, 20 and 40 μg/ml) of DHMEQ for 16 h. Both 20 and 40 μg/ml DHMEQ inhibited NF-κB activation in HUT-102 cells to a level that was approximately 50% of that in control cells. MOLT-4 cells were unaffected by DHMEQ (Fig. 1B). It is well established that HTLV-I Tax can activate the NF-κB pathway [5,6]. Therefore, to clarify the effect of DHMEQ on Tax, we analyzed NF-κB activity and *tax* expression in HUT-102 cells after treatment with 20 μg/ml DHMEQ for various periods. DHMEQ inhibited NF-κB activity to a level that was approximately 75% of that in control cells after 2 h of treatment (Fig. 1C, upper panel). This level was the same as that of MOLT-4 cells, and the inhibition was maintained even after 8 h. However, DHMEQ did not affect transcription from *tax* under the same conditions (Fig. 1C, lower panel). These results indicated that DHMEQ inhibits NF-κB activation in HUT-102 cells via a pathway that is not activated by Tax.

We then analyzed the effects of DHMEQ on the cellular distribution of the NF-κB components, p50 and p65, using indirect immunofluorescence. DHMEQ inhibited the nuclear localization of both p50 and p65 in HUT-102 cells.

in which these proteins show constitutive nuclear distribution in the absence of DHMEQ (Fig. 1D). In MOLT-4 cells, these proteins were distributed in the cytoplasm with or without DHMEQ treatment.

3.2. DHMEQ induces apoptosis of HUT-102 cells

HUT-102 cells were cultured with various concentrations (0–40 μg/ml) of DHMEQ for 0, 24 and 48 h to determine its effect on cell growth and survival. Cultivation with DHMEQ suppressed cell growth in a dose- and time-dependent manner, as assessed by the MTS assay (Fig. 2A). DHMEQ at >20 μg/ml suppressed growth by 50%. HTLV-I p19 in cell suspensions was also reduced by DHMEQ at 20 and 40 μg/ml for 16 h (Fig. 2B). To examine whether DHMEQ induces apoptosis. thereby accounting for the observed cell growth inhibition. apoptotic nuclei were counted in cells treated with 20 and 40 μg/ml DHMEQ and subsequently stained with Hoechst 33342. Significant apoptosis was measured in HUT102 cells. in contrast to the control MOLT-4 cells (Fig. 2C).
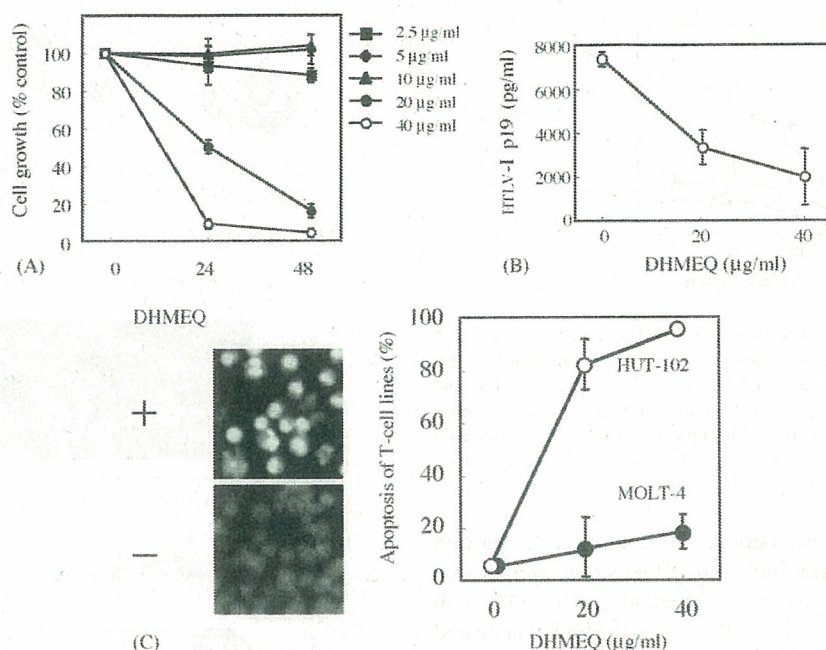
Fig. 2. DHMEQ reduces cell growth and induces apoptosis in HUT-102 cells. Cells were cultured with or without DHMEQ for 48 h. (A) Cell growth at different DHMEQ concentrations was assessed by the MTS method and is expressed as a percentage of the control (vehicle-treated). The data represent the mean ± standard deviation. (B) HTLV-I p19 gag protein in supernatants of cells treated with 20 or 40 µg/ml DHMEQ for 16 h. Data represent the mean ± standard deviation. (C) Induction of apoptosis of HUT102 cells by DHMEQ. The cells were fixed and stained with Hoechst 33342. At least 1000 stained cells were counted and assessed as apoptotic or non-apoptotic. MOLT-4 cells served as the control.

3.3. In vivo treatment of subcutaneous HUT-102 tumors with DHMEQ

To evaluate the efficacy of DHMEQ in vivo, SCID mice were inoculated with HUT-102 cells. These mice were then divided into three groups: vehicle-treated controls ($n = 7$), mice treated intraperitoneally (i.p.) with DHMEQ ($n = 7$) and mice treated subcutaneously (s.c.) with DHMEQ directly into the site of cell inoculation ($n = 8$). The tumors grew rapidly in control mice during the 2 weeks after inoculation. After 28 days, tumors in control mice encompassed the whole cervical area and were also found in forefeet (Fig. 3A,
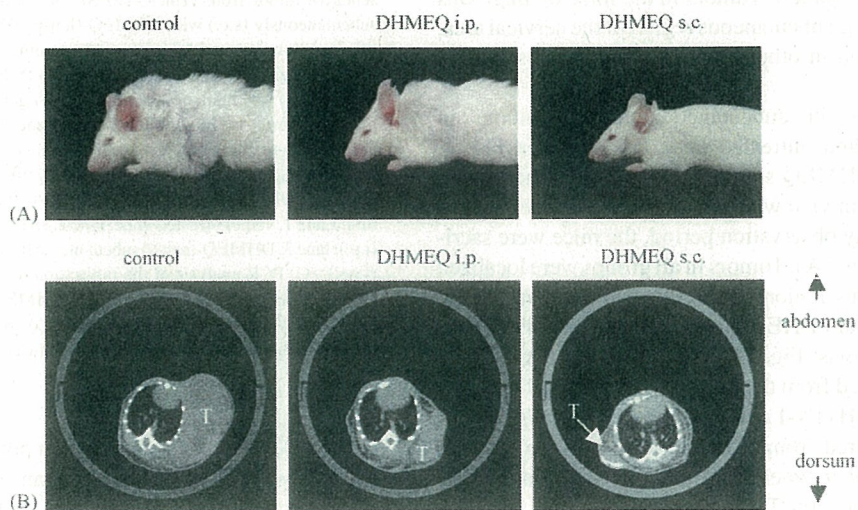

Fig. 3. Effect of DHMEQ on growth of HUT-102 cells in SCID mice. HUT-102 cells (5×10^7 per mouse) were inoculated subcutaneously into SCID mice in which NK cell activity had been eliminated. Mice were treated with vehicle or DHMEQ (12 mg/kg daily) intraperitoneally (i.p.) or subcutaneously (s.c., i.e., directly into the site of cell inoculation). (A) Images of vehicle-treated mice (left), i.p. DHMEQ-treated mice (middle), and s.c. DHMEQ-treated mice (right). (B) Mice were monitored using an X-ray CT scanner 12 days after cell inoculation to examine whether inoculated cells migrated to other sites or formed tumors outside of the cell inoculation site. T indicates the tumor.
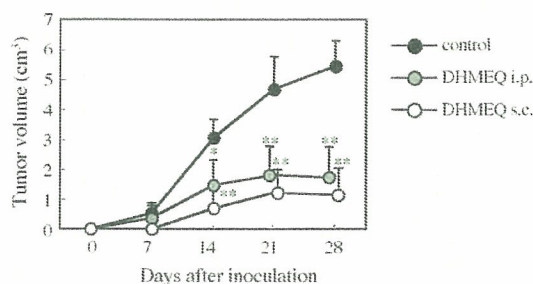
Fig. 4. Serial changes in tumor volume in DHMEQ-treated and untreated mice. The experiment was identical to that in Fig. 3. Tumor volumes were determined as described in Section 2. Data represent the average values and standard deviation for each group: vehicle-treated control mice ($n = 7$), mice treated with DHMEQ intraperitoneally (i.p.) ($n = 7$), and mice treated with DHMEQ subcutaneously (s.c.)—directly into the site of cell inoculation ($n = 8$). [*]$P < 0.05$ vs. control. [**]$P < 0.01$ vs. control.

left panel). During this period, the control mice showed signs of severe disease, including piloerection, weight loss and cachexia. In contrast, mice treated intraperitoneally with DHMEQ had small tumors in the cervical area but appeared generally healthy (Fig. 3A, middle). In mice treated subcutaneously (directly into tumor sites) with DHMEQ, the tumors observed in the cervical area were smaller than those in the group treated with DHMEQ intraperitoneally, and none of the mice showed clinical signs of imminent death (Fig. 3A, right panel).

To examine whether the inoculated tumor cells translocated to other sites or formed tumors outside of the site of cell inoculation, we monitored the mice using an X-ray CT scanner 12 days after cell inoculation (Fig. 3B). Mice treated subcutaneously with DHMEQ did not have palpable tumors; however, a small residual tumor was evident by CT scanning (Fig. 3B, right panel). Tumors in the mice of all groups were localized in the subcutaneous region of the cervical area, and were not found in other organs during the observation period.

Serial changes in subcutaneous tumor volume in DHMEQ-treated and untreated mice are shown in Fig. 4. Treatment with DHMEQ significantly inhibited the growth of HUT-102 cells in vivo with no obvious adverse effects.

After the 28-day observation period, the mice were sacrificed on day 30 (Fig. 5A). Tumors in all groups were localized in the subcutaneous region of the cervical area, and histological examination of HE-stained sections identified these tumors as lymphomas (Fig. 5A, right). To confirm that these tumors were derived from the inoculated cells, PCR was performed to detect HTLV-I *tax* and human *β-globin*. All of the tumors recovered from the mice were positive for both genes (Fig. 5B, upper panel). Furthermore, we examined the expression level of viral Tax by western blotting. Tax was detected in tumors of all groups as a specific band of about 40 kDa (Fig. 5B, lower panel).

To detect infiltration of inoculated cells into various organs, genomic DNA extracted from each organ was subjected to PCR using primers specific for HTLV-I *tax* and
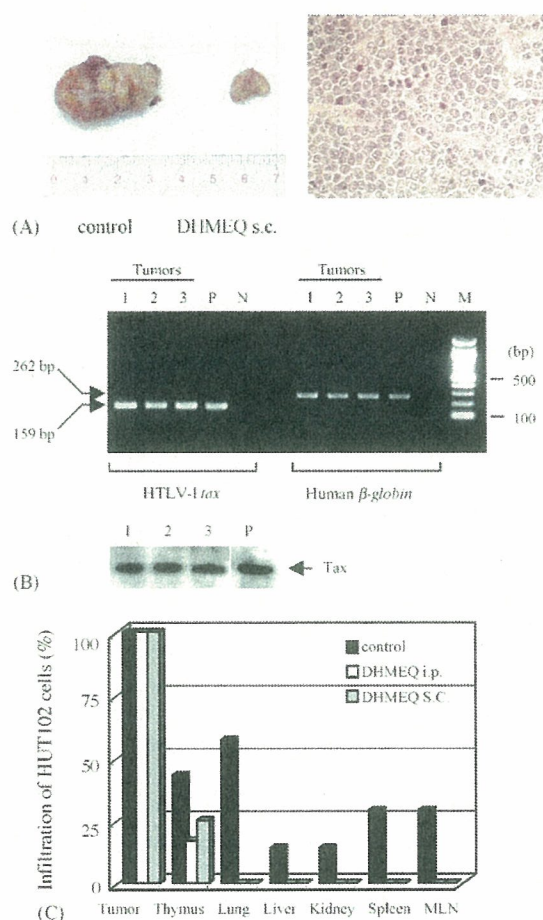

Fig. 5. Autopsy of DHMEQ-treated and untreated mice. Tumors were excised on day 30 after cell inoculation. (A) The images show a representative tumor from vehicle-treated control mice and from mice treated subcutaneously (s.c.) with DHMEQ (left panel). These tumors were identified as lymphomas by histological examination with HE-staining (right panel). Original magnification. ×100. (B) PCR analysis to detect HTLV-I *tax* (159 bp) and human *β-globin* (262 bp) genes showed tumors that had originated from HTLV-I-infected cells. Lane 1, vehicle-treated mice; lane 2, DHMEQ-treated intraperitoneally (i.p.); lane 3, DHMEQ-treated subcutaneously (s.c.); P. HUT-102 cells; N. negative; M. 100-bp ladder marker (upper panel). Tax was detected in tumors of all groups by western blotting. Lane 1. vehicle-treated mice; lane 2. DHMEQ-treated intraperitoneally (i.p.); lane 3. DHMEQ-treated subcutaneously (s.c.); P. HUT-102 cells (lower panel). (C) PCR analysis of the infiltration of inoculated cells into various organs in mice treated with or without DHMEQ. Primers were specific for either HTLV-I *tax* or human *β-globin*. The organs in which both genes were detected were considered positive. MLN. mesenteric lymph node.

human *β-globin*. Organs in which both genes were detected were considered positive. All organs tested were positive in the control mice (Fig. 5C). In DHMEQ-treated mice, only the thymus was positive in 17% of the intraperitoneal and 25% of the subcutaneous groups, whereas all the other organs were negative. Taken together, these data suggest that DHMEQ inhibits tumor growth and infiltration of HUT-102 cells to various organs in this SCID mouse model of ATL.

4. Discussion

In this report we have demonstrated that the HTLV-I-infected T-cell line, HUT-102, one of the most commonly used cell lines for HTLV-I studies, is sensitive to a novel NF-κB inhibitor, DHMEQ, both in vitro and in vivo. In vitro, DHMEQ is very effective at blocking constitutive NF-κB activity and inducing apoptosis in cells [11–13]. This agent did not significantly affect the viability of the non-infected T-cell line, MOLT-4. Most of the NF-κB inhibitors used for ATL preliminary therapy block either the phosphorylation [4,17] or proteasomal degradation [18–20] of IκBα. In contrast, DHMEQ targets the translocation of p65 into the nucleus [11], an activity downstream of IκB kinase, which is the target of IκB phosphorylation or proteasome inhibitors [21]. Based on this observation, we suggest that DHMEQ is more specific than other NF-κB inhibitors that have been previously reported.

Few studies have been reported that permit comparison of the effect of new therapeutic agents for ATL, both in vitro and in vivo, using the same cell lines [19,22]. Satou et al. [19] reported that the proteasome inhibitor, bortezomib, inhibits the growth of the HTLV-I-infected cell line, ED(−) (Tax-negative), both in vitro and in vivo. However, tumor size was measured only up to 10 days after cell inoculation of treated mice and in control mice. We speculate that the tumor size did not reach a plateau until after 10 days. Mori et al. [22] demonstrated that the histone deacetylase inhibitor, FR901228, also inhibits the growth of HUT-102 cells in vitro and in vivo. In their animal model, the system was useful for directly measuring in vivo antitumor effects, but infiltration of cells into other organs was not measured.

The infiltration of ATL cells into various organs is well documented in ATL patients. In the present study, SCID mice were treated with the anti-murine IL-2R β chain antibody, TM-β1, to eliminate NK activity [14]. This treatment prompted tumor growth and infiltration of injected cells to various organs. This SCID mouse model is thus useful for measuring the effects of drugs on both primary tumor growth as well as ATL cell infiltration of organ systems. Using this model, we showed that DHMEQ inhibits not only tumor formation but also infiltration of HUT-102 cells into various organs except thymus. We speculate that thymus is the first infiltrated organ and that these infiltrating cells subsequently migrate to other organs in this mouse model.

We recently reported that age is a critical factor influencing tumor formation and death in SCID mice injected intraperitoneally with the HTLV-I-transformed cell line, MT-2 [23]; furthermore, DHMEQ reduces mortality in this mouse model [24]. However, when SCID mice lacking natural killer cell activity were inoculated subcutaneously with MT-2 cells, no tumors were found. The discrepancy in mortality rates and tumor formation between MT-2 and HUT-102 cells may reflect differences in cytokine production. Further analysis of this discrepancy may help to establish new animal models of ATL.

Our current results demonstrate that DHMEQ not only inhibits tumor cell growth in vitro but also inhibits tumor formation and organ infiltration in vivo. Furthermore, DHMEQ does not show any apparent side effects in vivo. These results suggest that this novel NF-κB inhibitor has potential as an antitumor agent for ATL patients.

References

[1] Poiesz BJ, Ruscetti FW, Gazdar AF, Bunn PA, Minna JD, Gallo RC. Detection and isolation of type C retrovirus particles from fresh and cultured lymphocytes of a patient with cutaneous T cell lymphoma. Proc Natl Acad Sci USA 1980;77:7415–9.

[2] Hinuma Y, Nagata K, Hanaoka M, Nakai M, Matsumoto T, Kinoshita KI, et al. Adult T cell leukemia: antigen in an ATL cell line and detection of antibodies to the antigen in human sera. Proc Natl Acad Sci USA 1981;78:6476–80.

[3] Mori N, Fujii M, Ikeda S, Yamada Y, Tomonaga M, Ballard DW, et al. Constitutive activation of NF-κB in primary adult T cell leukemia cells. Blood 1999;93:2360–8.

[4] Mori N, Yamada Y, Ikeda S, Yamasaki Y, Tsukasaki K, Tanaka Y, et al. Bay 11-7082 inhibits transcription factor NF-kappaB and induces apoptosis of HTLV-I-infected T-cell lines and primary adult T-cell leukemia cells. Blood 2002;100:1828–34.

[5] Yamaoka S, Courtois G, Bessia C, Whiteside ST, Weil R, Agou F, et al. Complementation cloning of NEMO, a component of the IkappaB kinase complex essential for NF-kappaB activation. Cell 1998;93:1231–40.

[6] Sun SC, Ballard DW. Persistent activation of NF-kappaB by the tax transforming protein of HTLV-1: hijacking cellular IkappaB kinases. Oncogene 1999;18:6948–58.

[7] Hironaka N, Mochida K, Mori N, Maeda M, Yamamoto N, Yamaoka S. Tax-independent constitutive IkappaB kinase activation in adult T-cell leukemia cells. Neoplasia 2004;6:266–78.

[8] Watanabe M, Ohsugi T, Shoda M, Ishida T, Aizawa S, Maruyama-Nagai M, et al. Dual targeting of transformed and untransformed HTLV-1-infected T-cells by DHMEQ, a potent and selective inhibitor of NF-kB, as a strategy for chemoprevention and therapy of adult T cell leukemia. Blood, in press, http://www.bloodjournal.org/cgi/content/abstract/2004-09-3646v1.

[9] Matsumoto N, Ariga A, To-e S, Nakamura H, Agata N, Hirano S, et al. Synthesis of NF-kappaB activation inhibitors derived from epoxyquinomicin C. Bioorg Med Chem Lett 2000;10:865–9.

[10] Matsumoto N, Iinuma H, Sawa T, Takeuchi T, Hirano S, Yoshioka T, et al. Epoxyquinomicins A, B, C and D, new antibiotics from Amycolatopsis. II. Effect on type II collagen-induced arthritis in mice. J Antibiot (Tokyo) 1997;50:906–11.

[11] Ariga A, Namekawa J, Matsumoto N, Inoue J, Umezawa K. Inhibition of tumor necrosis factor-α-induced nuclear translocation and activation of NF-κB by dehydroxymethylepoxyquinomicin. J Biol Chem 2002;277:24625–30.

[12] Kikuchi E, Horiguchi Y, Nakashima J, Kuroda K, Oya M, Ohigashi T, et al. Suppression of hormone-refractory prostate cancer by a novel nuclear factor kappaB inhibitor in nude mice. Cancer Res 2003;63:107–10.

[13] Watanabe M, Dewan MZ, Okamura T, Sasaki M, Itoh K, Higashihara M, et al. A Novel NF-κB inhibitor DHMEQ selectively targets constitutive NF-κB activity and induces apoptosis of multiple myeloma cells in vitro and in vivo. Int J Cancer 2005;114:32–8.

[14] Tanaka T, Kitamura F, Nagasaka Y, Kuida K, Suwa H, Miyasaka M. Selective long-term elimination of natural killer cells in vivo by an anti-interleukin 2 receptor beta chain monoclonal antibody in mice. J Exp Med 1993;178:1103–7.

[15] Saiki RK, Gelfand DH, Stoffel S, Scharf SJ, Higuchi R, Horn GT, et al. Primer-directed enzymatic amplification of DNA with a thermostable DNA polymerase. Science 1988;239:487–91.

[16] Ohsugi T, Ishibashi K, Shingu M, Nomura T. Engraftment of HTLV-I-transformed human T cell line into SCID mice with NK cell function. J Vet Med Sci 1994;56:601–3.

[17] Dewan MZ, Terashima K, Taruishi M, Hasegawa H, Ito M, Tanaka Y, et al. Rapid tumor formation of human T cell leukemia virus type 1-infected cell lines in novel NOD-SCID/γc^{null} mice: suppression by an inhibitor against NF-κB. J Virol 2003;77:5286–94.

[18] Tan C, Waldmann TA. Proteasome inhibitor PS-341, a potential therapeutic agent for adult T cell leukemia. Cancer Res 2002;62:1083–6.

[19] Satou Y, Nosaka K, Koya Y, Yasunaga JI, Toyokuni S, Matsuoka M. Proteasome inhibitor, bortezomib, potently inhibits the growth of adult T-cell leukemia cells both in vivo and in vitro. Leukemia 2004;18:1357–63.

[20] Mitra-Kaushik S, Harding JC, Hess JL, Ratner L. Effects of the proteasome inhibitor PS-341 on tumor growth in HTLV-1 Tax transgenic mice and Tax tumor transplants. Blood 2004;104:802–9.

[21] Epinat JC, Gilmore TD. Diverse agents act at multiple levels to inhibit the Rel/NF-κB signal transduction pathway. Oncogene 1999;18:6896–909.

[22] Mori N, Matsuda T, Tadano M, Kinjo T, Yamada Y, Tsukasaki K, et al. Apoptosis induced by the histone deacetylase inhibitor FR901228 in human T-cell leukemia virus type 1-infected T-cell lines and primary adult T-cell leukemia cells. J Virol 2004;78:4582–90.

[23] Ohsugi T, Yamaguchi K, Kumasaka T, Ishida T, Horie R, Watanabe T, et al. Rapid tumor death model for evaluation of new therapeutic agents for adult T-cell leukemia. Lab Invest 2004;84:263–6.

[24] Ohsugi T, Horie R, Kumasaka T, Ishida A, Ishida T, Yamaguchi K, et al. In vivo antitumor activity of the NF-kB inhibitor dehydroxymethylepoxyquinomicin in a mouse model of adult T-cell leukemia. Carcinogenesis, in press. http://carcin.oxfordjournals.org/cgi/content/abstract/bgi095v1.

LC16m8, a Highly Attenuated Vaccinia Virus Vaccine Lacking Expression of the Membrane Protein B5R, Protects Monkeys from Monkeypox

Masayuki Saijo,[1]* Yasushi Ami,[2] Yuriko Suzaki,[2] Noriyo Nagata,[3] Naoko Iwata,[3] Hideki Hasegawa,[3] Momoko Ogata,[1] Shuetsu Fukushi,[1] Tetsuya Mizutani,[1] Tetsutaro Sata,[3] Takeshi Kurata,[3] Ichiro Kurane,[1] and Shigeru Morikawa[1]

Special Pathogens Laboratory, Department of Virology 1,[1] Laboratory of Animal Experimentation,[2] and Laboratory of Infectious Disease Pathology, Department of Pathology,[3] National Institute of Infectious Diseases, Tokyo, Japan

The potential threat of smallpox as a bioweapon has led to the production and stockpiling of smallpox vaccine in some countries. Human monkeypox, a rare but important viral zoonosis endemic to central and western Africa, has recently emerged in the United States. Thus, even though smallpox has been eradicated, a vaccinia virus vaccine that can induce protective immunity against smallpox and monkeypox is still invaluable. The ability of the highly attenuated vaccinia virus vaccine strain LC16m8, with a mutation in the important immunogenic membrane protein B5R, to induce protective immunity against monkeypox in nonhuman primates was evaluated in comparison with the parental Lister strain. Monkeys were immunized with LC16m8 or Lister and then infected intranasally or subcutaneously with monkeypox virus strain Liberia or Zr-599, respectively. Immunized monkeys showed no symptoms of monkeypox in the intranasal-inoculation model, while nonimmunized controls showed typical symptoms. In the subcutaneous-inoculation model, monkeys immunized with LC16m8 showed no symptoms of monkeypox except for a mild ulcer at the site of monkeypox virus inoculation, and those immunized with Lister showed no symptoms of monkeypox, while nonimmunized controls showed lethal and typical symptoms. These results indicate that LC16m8 prevents lethal monkeypox in monkeys, and they suggest that LC16m8 may induce protective immunity against smallpox.

Three decades have passed since the global eradication of smallpox (variola). This eradication was made possible by the development of effective vaccinia virus vaccines (VVs), such as strains Lister and Dryvax. Unfortunately, we now face the potential threat of bioterrorism with variola virus, the causative agent of variola. This threat has led to the production and stockpiling of vaccinia virus-based vaccines in several countries. Human monkeypox (MPX), infection of humans with monkeypox virus (MPXV), is endemic to central and western Africa (18), and the first human MPX outbreaks outside Africa were reported in the United States in 2004 (6, 9, 30). Most human MPX patients in this outbreak acquired the virus from prairie dogs (*Cynomys* spp.) that became ill after contact with various exotic rodents shipped from Ghana, Africa (30). Therefore, VVs are still of great importance, although variola has already been eradicated.

LC16m8, a highly attenuated VV strain, was developed in the early 1970s by multiple passages in cell culture through a temperature-sensitive and low-virulence strain, LC16mO, from the original Lister strain (Elstree) (11, 36). LC16m8 forms smaller plaques than Lister in the chicken chorioallantoic membrane. LC16m8 is temperature sensitive, as demonstrated by the fact that LC16m8 does not grow well in primary rabbit kidney (PRK) cells cultured at 41°C, while Lister grows efficiently (36). The fact that LC16m8 grows efficiently in PRK

cells but not in African green monkey kidney (Vero) cells, while the parental strain Lister grows well in both cell lines, suggests that LC16m8 has a narrow host cell range, growing in a cell-selective manner (36).

We recently determined the complete genome sequences of LC16m8, the parental LC16mO strain, and the original Lister strain (GenBank accession no. AY678275, AY678277, and AY678276, respectively) (24). It was revealed that there was a single nucleotide deletion of guanosine (G) at the 274th position from the initiation codon in the membrane protein gene *B5R* (GenBank accession no. M55434 and AY678275) that generated a premature termination codon and truncated the B5R membrane protein of LC16m8 extracellular enveloped virions (EEV) at amino acid position 93. LC16m8 may possess nearly all the open reading frames corresponding to the VV strains Copenhagen and Lister except for the membrane protein B5R. Because Lister had no history of virus cloning, nucleotide polymorphisms were observed at more than 1,000 sites in the whole genome, indicating that it is difficult to make a simple comparison between the nucleotide sequences of LC16m8 and Lister. However, alignments of the EEV-related membrane proteins in LC16m8 and Lister indicated that there were only 1, 1, 1, and 2 amino acid differences in the EEV-related membrane proteins A36R, F13L, A56R, and A33R, respectively, and that the EEV-related membrane protein A34R of LC16m8 was identical to that of Lister. Although the genetic background responsible for the temperature sensitivity has not been elucidated, it has been confirmed that mutation in the membrane protein gene *B5R* is responsible for small-plaque formation and cell-selective growth of this strain (35).

---

* Corresponding author. Mailing address: Department of Virology 1, National Institute of Infectious Diseases, 4-7-1 Gakuen, Musashimurayama, Tokyo 208-0011, Japan. Phone: 81-42-561-0771, ext. 320. Fax: 81-42-561-2039. E-mail: msaijo@nih.go.jp.

LC16m8 has very low neurovirulence in animal models (11). More than 100,000 people were vaccinated with LC16m8 in Japan, but no LC16m8-associated adverse events such as serious complications and/or death were reported. The currently available VVs, such as strains Lister and Dryvax, are known to be efficacious. However, severe adverse events, such as encephalitis, encephalopathy, progressive and generalized vaccinia, ocular vaccinia virus infections, and cardiac dysfunction, have been reported for recipients and are of great concern (1, 2, 4, 10, 16, 22, 23, 25, 31, 33, 38). These observations suggest that LC16m8 is safer than the currently used VVs derived from bovine skin (20, 21). Thus, LC16m8 is considered a potentially useful replacement for the currently available VVs.

Unfortunately, the protective efficacy of LC16m8 against variola has not been evaluated, because variola had already been eradicated at the time of its development. LC16m8 lacks expression of the full-length membrane protein B5R, one of the most immunogenic proteins, because of a frameshift mutation in the membrane protein gene *B5R* (19, 35). It is expected that LC16m8 does not pass through the EEV stage in the viral life cycle, because the membrane protein B5R is essential in packaging the intracellular mature virion with the *trans*-Golgi membrane or endosomal cisternae to form intracellular enveloped virions (13, 32, 34) and this protein is also involved in the release of cell-associated enveloped virions from the cell surface to form EEV in cooperation with proteins A36R and A33R (17, 29). Furthermore, the membrane protein B5R induces protective neutralizing antibodies to EEV in vaccinia (8, 14, 15, 34). Recently, it was reported that LC16m8 induced protective immunity to vaccinia virus challenge in mice and rabbits (19, 24). However, the protective efficacy of LC16m8 against variola and human MPX has not been confirmed in humans.

If LC16m8 is as efficacious as Lister and Dryvax, it will be of great benefit to humans, because it is expected to induce much less severe VV-associated adverse events. A nonhuman-primate model for MPXV infections is expected to mimic natural variola virus infection in humans. In the present study, the protective efficacy of LC16m8 against MPX was evaluated in comparison with that of Lister VV in cynomolgus monkeys (*Macaca fascicularis*). The present study was performed to examine the protective efficacy of LC16m8 against variola in humans.

MATERIALS AND METHODS

Virus, vaccinia virus vaccines, and cells. MPXV strains Liberia and Zr-599, used in challenge experiments, and MPXV Congo-8, used in the neutralizing antibody assay, had been kept in the National Institute of Infectious Diseases. Strain Liberia was originally isolated from a patient with MPX in Liberia, and strain Zr-599 was from a patient with MPX in the Democratic Republic of Congo (formerly Zaire), suggesting that the former originated from West Africa and the latter from the Congo Basin. It is suggested that MPXV originating from West Africa is less virulent than MPXV originating from the Congo Basin (3). The virus was confirmed to be MPXV by determining the specific nucleotide sequence of the ATI gene of MPXV (28). The infectious dose of the virus was determined by plaque assays on Vero cells, which were purchased from the American Type Cell Collection (Manassas, VA). Vero cells were grown in Eagle's minimum essential medium supplemented with penicillin G and streptomycin and with 5% fetal bovine serum (MEM-5FBS). LC16m8 vaccine was produced by the Chiba Serum Research Institute, Chiba, Japan, and Lister vaccine was produced by the Kitasato Research Institute, Kanagawa, Japan. The titers of the two vaccines were higher than 1 × 10⁸ PFU/ml.

Nonhuman primates and vaccination. One male and 14 female cynomolgus monkeys (*Macaca fascicularis*), aged 3 to 4 years and weighing 2,180 to 3,100 g, were used in the experiments (Table 1). These monkeys were born and raised in the Tsukuba Primate Center for Medical Research, National Institute of Infectious Diseases, Tsukuba, Japan. They were assigned to six groups as shown in Table 1: group IN-Naïve, consisting of naïve monkeys challenged intranasally with MPXV (monkeys 4595 and 4596), group IN-Lister, consisting of monkeys immunized with Lister and challenged intranasally with MPXV (monkeys 4597, 4598, and 4599), group IN-LC16m8 (monkeys 4600, 4601, and 4602), group SC-Naïve, consisting of naïve monkeys challenged subcutaneously with MPXV (monkeys 4651 and 4653), group SC-Lister (monkeys 4575 and 4576), and group SC-LC16m8 (monkeys 4577, 4525, and 4526). Monkeys were immunized with each of the vaccines by the multiple-puncture method with standard bifurcated needles in the same way as immunization is performed for humans. Briefly, a bifurcated needle holding a drop of vaccine was pressed more than 15 times into the skin at the vaccination site.

Assays of IgG antibody. Levels of vaccinia virus-specific antibody were measured by an enzyme-linked immunosorbent assay (ELISA) using the entire vaccinia virus proteins as antigens, as reported previously, except for the secondary antibody conjugated with horseradish peroxidase (24). The secondary antibody was a goat anti-human immunoglobulin G (IgG) antibody conjugated with horseradish peroxidase purchased from Zymed Laboratories (South San Francisco, CA).

Neutralizing antibody assay. Levels of neutralizing antibody to MPXV Congo-8 in the plasma samples were measured as reported previously with some modifications (12). Briefly, about 30 PFU of MPXV strain Congo-8 in 100 μl of MEM-2FBS was mixed with 100 μl of serially diluted heat-inactivated plasma samples and incubated at 4°C overnight. The mixtures were inoculated into Vero cell monolayers seeded in a 24-well culture plate and were incubated for 2 h for adsorption. The inocula were then removed, and the cells were cultured with MEM-2FBS supplemented with 0.5% methylcellulose. After a 3-day incubation, plaque numbers were counted. The neutralizing antibody titer was defined as the reciprocal of the dilution level at which the plaque number decreased to less than 50% of that in the control.

Cytokine assays. The concentrations of tumor necrosis factor alpha (TNF-α), gamma interferon (IFN-γ), interleukin-2 (IL-2), IL-4, IL-6, and IL-10 in sera were determined using rhesus monkey TNF-α, monkey IFN-γ, rhesus monkey IL-2, monkey IL-4, human IL-6, and rhesus monkey IL-10 (BioSource International Inc., Camarillo, CA), respectively, according to the manufacturer's instructions.

Virus isolation from PBMCs or buffy coat fraction. Virus was isolated using Vero cells from peripheral blood mononuclear cells (PBMCs) and buffy coat fractions obtained from monkeys inoculated intranasally and subcutaneously, respectively. PBMCs were isolated from peripheral blood by the Ficoll centrifugation method. Aliquots of 10⁶ PBMCs were cocultivated with Vero cells in MEM-2FBS for 2 weeks, when PBMCs were used. The whole buffy coat fraction collected by centrifugation of 4 ml of peripheral blood was washed twice with a phosphate-buffered saline solution and then cocultivated with Vero cells as described above. When a cytopathic effect was observed in cell culture, the cytopathic effect agent was confirmed to be MPXV by an indirect immunofluorescence assay with an anti-vaccinia virus antibody prepared in our laboratory and by amplification of the ATI gene and sequencing of the amplicon (28). Furthermore, the plaque number was also counted.

Determination of MPXV loads in total peripheral blood by quantitative PCR. DNAs were isolated from total peripheral blood using a Viral Nucleic Acid purification kit (Roche Diagnostics, Mannheim, Germany) according to the supplier's instructions. The primers and probes were designed based on the specific ATI gene on the MPXV genome. The sequences of primers and probes were as follows: forward primer, 5'-GAGATTAGCAGACTCCAA-3'; fluorescein probe, 5'-GCAGTCGTTCAACTGTATTTCAAGATCTGAGAT-3'-fluorescein; LCRed640 probe, 5'-LCRed640-CTAGATTGTAATCTCTGTAGCAT TTCCACGGC-3'-phosphorylation; reverse primers, 5'-TCTCTTTTCCATATC AGC-3' for amplification of the MPXV Liberia genome and 5'-GATTCAATT TCCAGTTTGTAC-3' for amplification of the MPXV Zr-599 genome. The internal controls for determination of viral genome copy numbers of MPXV Liberia and MPXV Zr-599 were pGEM-T Easy vectors (Promega Cooperation, Madison, WI) carrying the ATI gene of MPXV strain Liberia or Zr-599, respectively, and were included in each quantitative real-time PCR (qPCR) assay. The reverse primer sequences were designed according the nucleotide sequences of the ATI genes of MPXV Liberia and Zr-599. Amplification conditions were 95°C for 10 min, followed by 40 cycles of 95°C for 10 s, 57°C for 10 s, and 72°C for 6 s, and a melting reaction.

TABLE 1. Characteristics, MPX-associated symptoms, and viremia in mock-immunized monkeys and those
immunized with Lister or LC16m8

Group	ID[a]	Vaccination	Sex[b] (wt [g])	MPXV challenge strain (route,[c] dose [PFU])	Virus isolation[d] (no. of plaques at the indicated day of collection)	MPX-associated symptoms		
						Symptom(s) at the site of MPXV inoculation	No. of papulovesicular lesions	Outcome
Expt 1								
IN-Naïve	4595	Mock	F (2,500)	Liberia (IN, 10^6)	Positive (20 at day 4, 10 at day 6, 10 at day 8)	Rhinorrhea	10	Survival
	4596		F (2,320)		Positive (10 at day 6, 10 at day 13)	Rhinorrhea	16	Survival
IN-Lister	4597	Lister	F (2,360)		Negative	None	0	Survival
	4598		F (2,580)		Negative	None	0	Survival
	4599		F (2,700)		Negative	None	0	Survival
IN-LC16m8	4600	LC16m8	F (2,650)		Negative	None	0	Survival
	4601		F (2,800)		Negative	None	0	Survival
	4602		F (2,700)		Negative	None	0	Survival
Expt 2								
SC-Naïve	4651	Mock	F (2,560)	Zr-599 (SC, 10^6)	Positive (4 at day 3, 5 at day 7, 33 at day 9, 30 at day 14)	Erythema, papulovesicles, ulcer	390	Death
	4653		M (3,100)		Positive (176 at day 3, 18 at day 7, 3 at day 9, 23 at day 11, 9 at day 14, 3 at day 18)	Erythema, papulovesicles, ulcer	1,150	Death
SC-Lister	4575	Lister	F (2,980)		Negative	None	0	Survival
	4576		F (3,100)		Negative	None	0	Survival
SC-LC16m8	4577	LC16m8	F (2,640)		Positive (1 at day 3)	Erythema	0	Survival
	4525		F (2,180)		Positive (7 at day 3, 1 at day 6)	Erythema, papulovesicles, ulcer	0	Survival
	4526		F (2,730)		Negative	Erythema, papulovesicles, ulcer	0	Survival

[a] ID, monkey identification number.
[b] F, female; M, male.
[c] IN, intranasal inoculation; SC, subcutaneous inoculation.
[d] Positive or negative, MPXV was or was not isolated, respectively, during the observation period from challenge to sacrifice. In experiment 1, the intranasal inoculation model, virus isolation was attempted from aliquots of 10^6 purified PBMCs collected from monkeys on days 0, 2, 4, 6, 8, 10, 13, 16, and 20 after virus challenge. In experiment 2, the subcutaneous inoculation model, virus isolation was attempted from the buffy coat fractions collected from 4-ml aliquots of total peripheral blood collected on days 0, 3, 7, 9, 11, 14, and 18.

Challenge with MPXV. All the challenge experiments with MPXV were conducted in a highly contained laboratory at the National Institute of Infectious Diseases, Tokyo, Japan. The monkeys that were mock immunized or immunized with vaccines (Lister and LC16m8) were anesthetized and either inoculated intranasally with 0.5 ml of a virus solution containing 1×10^6 PFU of MPXV strain Liberia by using an atomizer (Keytron Co., Tokyo, Japan) to atomize the virus solution or inoculated subcutaneously with 0.5 ml of a virus solution containing 1×10^6 PFU of MPXV strain Zr-599. Blood samples were collected every week after immunization up to the time of challenge. After the challenge, blood was drawn every 2 to 4 days. Clinical manifestations, such as volume of food and water consumed, the appearance of feces, etc., were observed every day. When monkeys were anesthetized for drawing of blood, the skin surface was observed carefully, and body temperature and weight were measured.

Schedule for immunization and challenge. In the present study, day zero was defined as the day on which monkeys were challenged with MPXV. All of the monkeys were challenged with MPXV at 5 weeks after immunization. Monkeys were challenged with MPXV (strain Liberia or Zr-599) on day zero and were observed for about 3 weeks.

Histopathological examination. After sacrifice under deep anesthesia using ketaral, skin, lymph nodes, brain, lungs, heart, liver, spleen, pancreas, kidneys, bladder, gastrointestinal organs, and genitourinary tract structures were excised, fixed in 10% formalin in phosphate-buffered saline, and embedded in paraffin. Macroscopic and histological examinations were performed on the excised tissues and organs. Paraffin sections, 4 μm thick, were stained with hematoxylin and eosin (H&E) and with Luxol-Fast Blue for the brain. Immunohistochemistry (IHC) for the MPXV antigens was performed using paraffin sections according

to the method described previously (26, 27). For detection of MPXV antigens, a rabbit anti-vaccinia virus serum was used.

RESULTS

Skin lesions after immunization with LC16m8 or Lister. Immunization with LC16m8 or Lister induced "vaccine take" (pustules, scabs, and scarring) as shown in Fig. 1. The lesions reached a maximum size at about 2 weeks after immunization. On day 13 postimmunization, the area was 27 ± 11 mm^2 with LC16m8, significantly smaller than the area of lesions induced by Lister (115 ± 65 mm^2) (Fig. 1B). The lesions induced by Lister were more exudative and granulomatous than those induced by LC16m8. Satellite lesions appeared with Lister but not with LC16m8. Pigmentation of the scars was apparent with Lister, but not with LC16m8, on day 28.

Protection of monkeys from intranasal MPXV challenge by immunization with LC16m8. The challenge experiment included six groups: (i) the IN-Naïve group, comprising two monkeys vaccinated with mock vaccine (negative control) and challenged intranasally with MPXV strain Liberia; (ii) the IN-

(A)

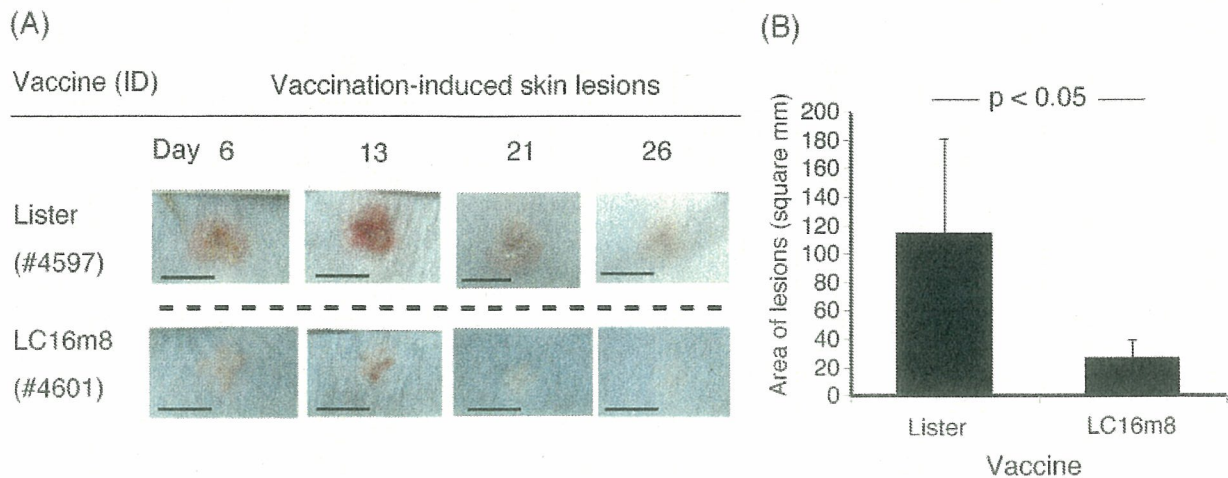Vaccine (ID)   Vaccination-induced skin lesions

(B)

FIG. 1. Local cutaneous lesions at the site (upper left arm) of vaccination with Lister or LC16m8. (A) Typical vaccine-induced local lesions on the designated days postimmunization. Bars, 10 mm. (B) Sizes (areas) of the vaccine-induced lesions with Lister ($n = 5$) or LC16m8 ($n = 6$), measured on day 13 and shown as averages and standard deviations.

Lister group, comprising three monkeys vaccinated with Lister and challenged intranasally with MPXV strain Liberia; (iii) the IN-LC16m8 group, comprising three monkeys vaccinated with LC16m8 and challenged intranasally with MPXV strain Liberia; (iv) the SC-Naïve group, comprising two monkeys vaccinated with mock vaccine (negative control) and challenged subcutaneously with MPXV strain Zr-599; (v) the SC-Lister group, comprising two monkeys vaccinated with Lister and challenged subcutaneously with MPXV strain Zr-599; and (vi) the SC-LC16m8 group, comprising three monkeys immunized with LC16m8 and challenged subcutaneously with MPXV Zr-599.

The identification numbers of the monkeys and their sex, weight, and vaccination histories are shown along with summarized results in Table 1. The monkeys were challenged intranasally with MPXV 5 weeks after mock immunization or immunization with VVs (Table 1, experiment 1). Body weight decreased sharply after challenge, by approximately 10%, in group IN-Naïve but not in group IN-Lister or IN-LC16m8 (Fig. 2). In the IN-Naïve group, symptoms including loss of appetite, rhinorrhea and conjunctival discharge, diarrhea, skin rash (papulovesicular and ulcerative lesions, as shown in Fig. 3A), irritability, and decreased activity appeared around day 10 after challenge and continued for approximately 5 days. All the MPX-associated symptoms disappeared by day 20 after challenge except for the skin lesions. All animals in the IN-Lister and IN-LC16m8 groups survived and showed no symptoms associated with MPXV infection.

Histopathological examinations of the nasal cavity were carried out at the inoculation site to compare the efficacies of the vaccines in conferring protection against MPXV challenge. In IN-Naïve monkeys, the structures of the mucous membranes were damaged due to necrosis, inflammatory cell accumulation was seen, and MPXV antigens were detected in the lesions. In contrast, the nasal structures of the mucous membranes were maintained, and no MPXV antigens were detected, in the IN-Lister and IN-LC16m8 groups. Inflammation in the mucous membranes was detected in the IN-LC16m8 group but not in the IN-Lister group (Fig. 4).

Protection of monkeys against lethal subcutaneous MPXV challenge by immunization with LC16m8. The efficacy of LC16m8 in the lethal MPXV infection model was then evaluated (Table 1, experiment 2). Subcutaneous infection with MPXV Zr-599 was fatal to nonimmunized monkeys in the SC-Naïve group (Table 1). Body weight was decreased by approximately 15% after challenge in the SC-Naïve group. However, the monkeys in the SC-Lister and SC-LC16m8 groups maintained their body weight (Fig. 2). Papulovesicular skin lesions appeared on day 7 after challenge in the SC-Naïve group; monkeys 4651 and 4653 showed 390 and 1,150 lesions, respectively. The symptoms of both of the monkeys in the SC-Naïve group were so severe that they were euthanized for ethical reasons. On the other hand, the monkeys in the SC-LC16m8 group did not develop any MPX-associated symptoms, except for local cutaneous lesions at the site of MPXV inoculation (Fig. 4). The lesions consisted of erythema, vesicles, and ulceration and were much milder than those for the SC-Naïve group. The SC-Lister group showed no MPX-associated symptoms, not even cutaneous lesions at the site of MPXV inoculation (Fig. 4).

Histopathological examination. All the monkeys were sacrificed for virological and histopathological examination 3 weeks after MPXV challenge. After intranasal inoculation, nodular and granulomatous lesions were detected in the lungs in the IN-Naïve group, while no lesions were detected in the lungs of any of the monkeys in the IN-Lister and IN-LC16m8 groups (Fig. 3A). IHC examination with an anti-vaccinia virus antibody revealed the presence of MPXV in the nodular lesions (Fig. 3A). Similar nodular lesions caused by MPXV were also detected in the pancreas of monkey 4595 in the IN-Naïve group (Fig. 3A). Macroscopic and histological examination revealed that the thymus, tonsil, and lymph node structures were affected by MPXV in the IN-Naïve monkeys. In contrast, no MPX-associated lesions were detected in any of the monkeys in the IN-Lister and IN-LC16m8 groups by histopathological examination.

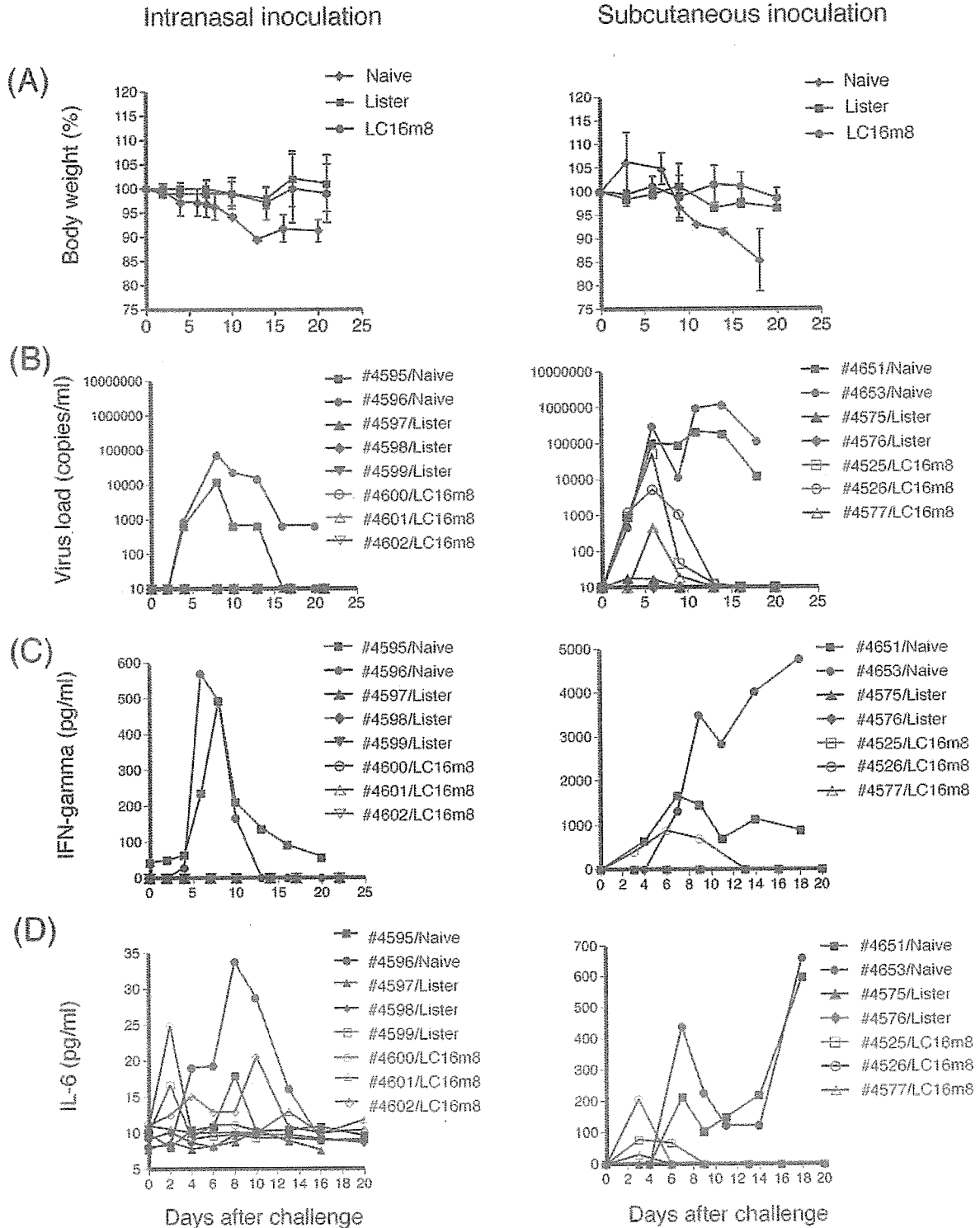After subcutaneous inoculation with MPXV, MPX-associ-

FIG. 2. Changes in body weight, MPXV loads in total peripheral blood, and cytokine responses. (A) Body weight expressed as a percentage of that measured at the time of MPXV challenge. (B) Viral loads in total peripheral blood as measured by qPCR. (C) IFN-γ response. (D) IL-6 response. Left and right panels show these indicators for monkeys challenged intranasally with MPXV strain Liberia and subcutaneously with MPXV Zr-599, respectively.
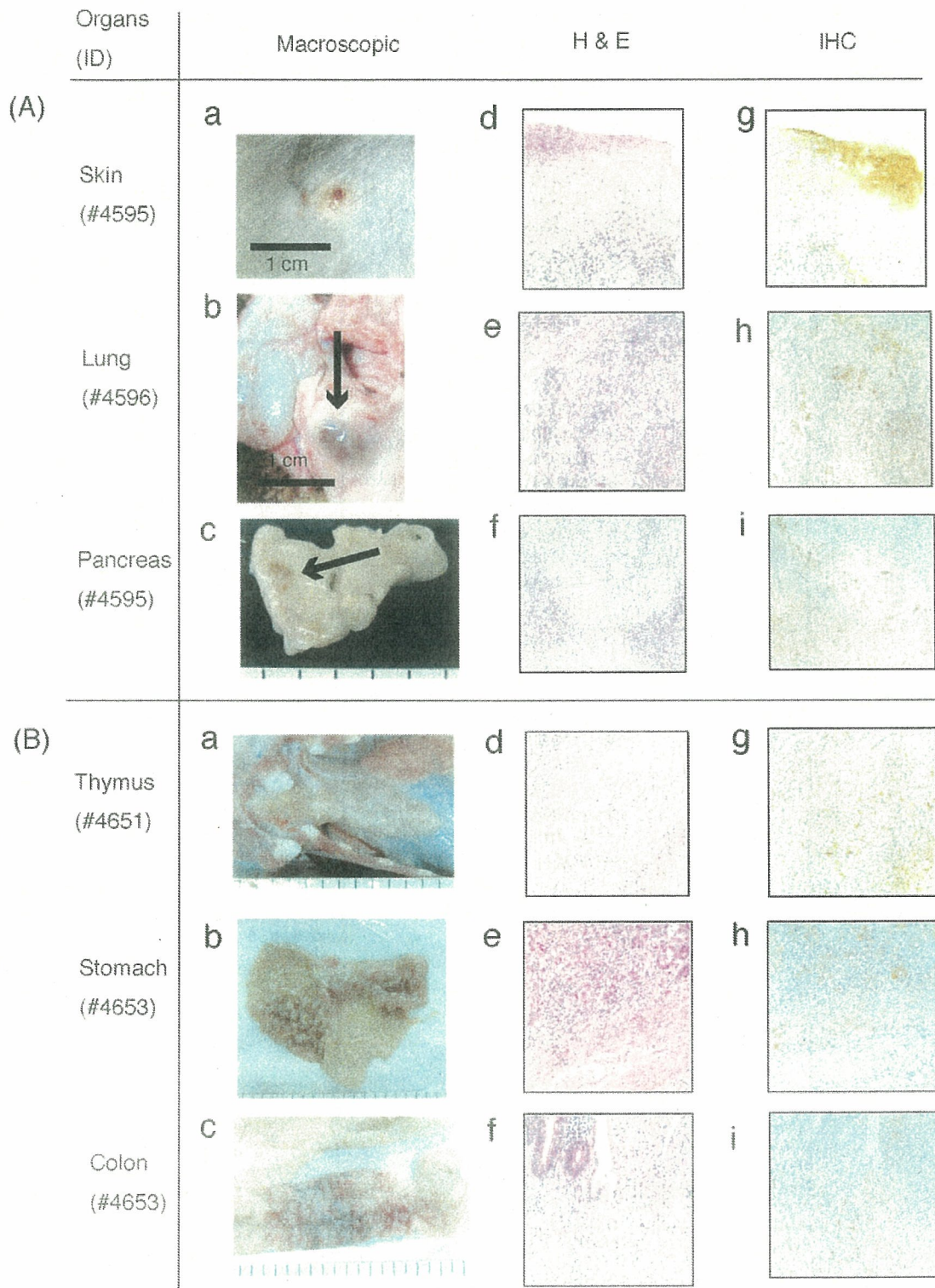
FIG. 3. Macroscopic and histological lesions observed in naïve monkeys infected with MPXV. (A) Macroscopic and histological lesions in the skin, lungs, and pancreas in the IN-Naïve group. Papulovesicular lesions were observed in the skin (a), and nodular and granulomatous lesions were present in the lungs (b) and pancreas (c). (d) The edges of the cutaneous lesions were characterized by epithelial cell swelling, epidermal hyperplasia, hyperkeratosis, necrosis, and infiltration of inflammatory cells. (e) Nodular and granulomatous lesions in the lungs were characterized by destruction of alveolar structures, necrosis, edema, proliferating fibroblasts, and infiltration of inflammatory cells. (f) Nodular and granulomatous lesions in the pancreas were characterized by extensive necrosis with infiltration of inflammatory cells and proliferating fibroblasts. (g to

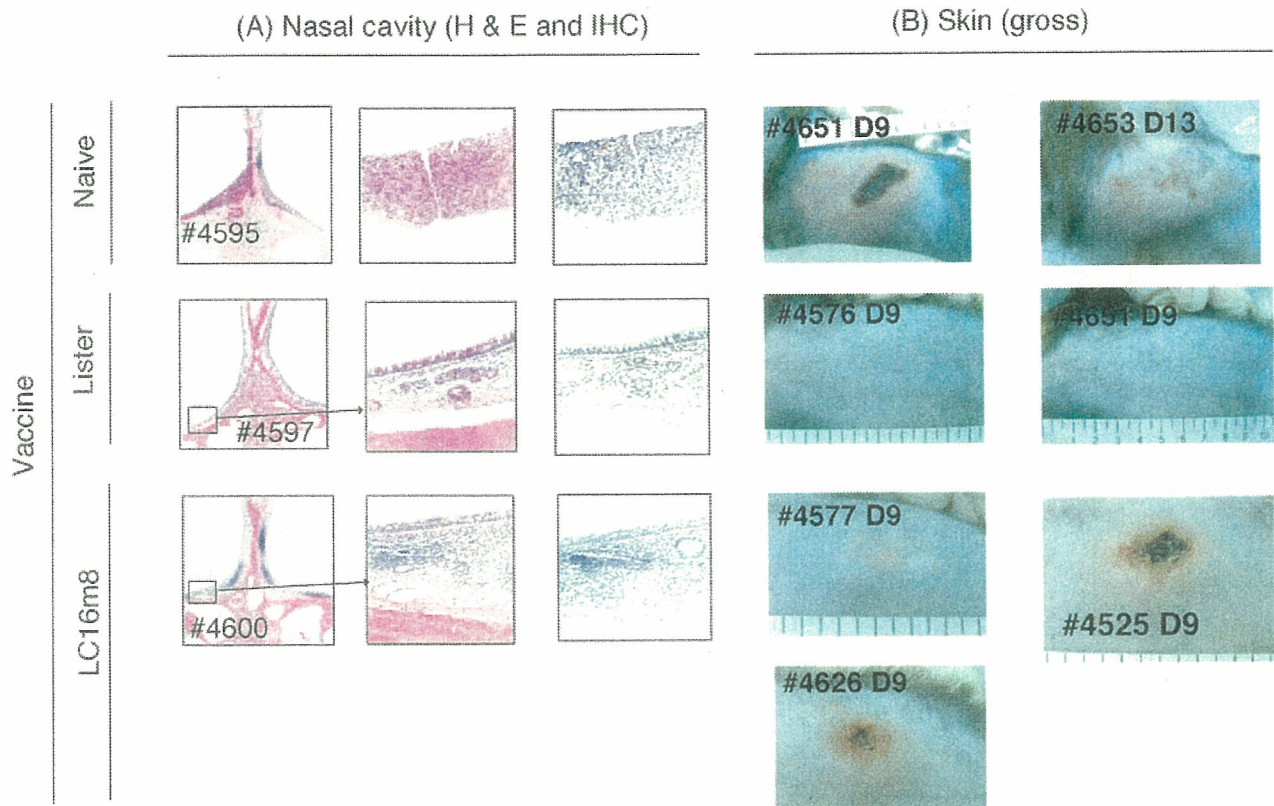## Lesions at the site of direct MPXV inoculation

FIG. 4. Histology of the nasal cavity caused by intranasal challenge with MPXV strain Liberia (A) and macroscopic lesions at the site of subcutaneous inoculation with MPXV strain Zr-599 (B). The identification numbers of monkeys are given. Analyses by H&E staining (A, low and high magnifications) revealed that the lesions of naïve monkey 4595 were characterized by destruction of mucous membrane structures, disappearance of mucosal epithelial cells resulting in ulcer formation, necrosis, and hyperplasia. MPXV antigens were present in the lesions. In contrast, the mucous membranes of the nasal cavity into which MPXV was inoculated in Lister-immunized monkey 4597 were normal, and MPXV antigens were not detected. Although the mucous membranes of the LC16m8-immunized monkey 4600 showed infiltration of inflammatory cells, the structure was maintained without necrosis. Furthermore, MPXV antigens were not detected. (B) Erythematous, vesicular, and ulcerative lesions appeared in the SC-Naïve group. The maximum diameter of the lesions exceeded 10 cm on day 14 postchallenge. In the SC-LC16m8 group, similar but milder lesions were observed, while no obvious lesions were detected at the site of inoculation in the SC-Lister group.

ated lesions were detected in the lymphoid systems (lymph nodes, thymus, and tonsils), respiratory tract structures (lung and trachea), digestive organs (stomach, small intestine, colon, rectum, and liver), urogenital tract (bladder, uterus, and ovary), or skin in the SC-Naïve group (Fig. 3B and 4B). On the other hand, no MPX-associated lesions were detected in any internal organs of any of the monkeys in the SC-Lister and SC-LC16m8 groups, except for skin lesions at the site of MPXV inoculation in the SC-LC16m8 group (Fig. 4B).

Laboratory findings and cytokine responses. C-reactive protein (CRP) levels were measured as an indicator of inflammation. CRP levels were significantly increased in groups IN-Naïve and SC-Naïve but not in any of the animals immunized with either vaccine (data not shown). Furthermore, lymphocytopenia and thrombocytopenia were also detected in mock-immunized naïve monkeys but were not apparent in any of the animals immunized with either vaccine (data not shown). The levels of IFN-γ, TNF-α, IL-2, IL-4, IL-6, and IL-10 in plasma

---

i) In these lesions, MPXV antigens were demonstrated by IHC analyses, indicating that they were caused by MPXV infection. (B) Macroscopic and histological lesions in the thymus, stomach, and colon in the SC-Naïve group. (a to c) Multiple nodular lesions were present in the thymus, and papilliform and granular lesions with hemorrhaging were seen in the lumens of the stomach and colon. (d) The lesions in the thymus were characterized by granulomatous inflammation and proliferation of fibrous tissue consisting of fibroblastic cells, histiocytes, and microvascular structures. (e) The histology in the stomach consisted of necrotic changes with inflammatory cells including neutrophils. (f) The submucosal area of the colon consisted of fibroblastic tissues with granulomatous inflammation characterized by infiltration of inflammatory cells. The mucosal membranes showed ulceration. (g to i) In these lesions, MPXV antigens were demonstrated by IHC analyses, indicating that they were caused by MPXV infection.
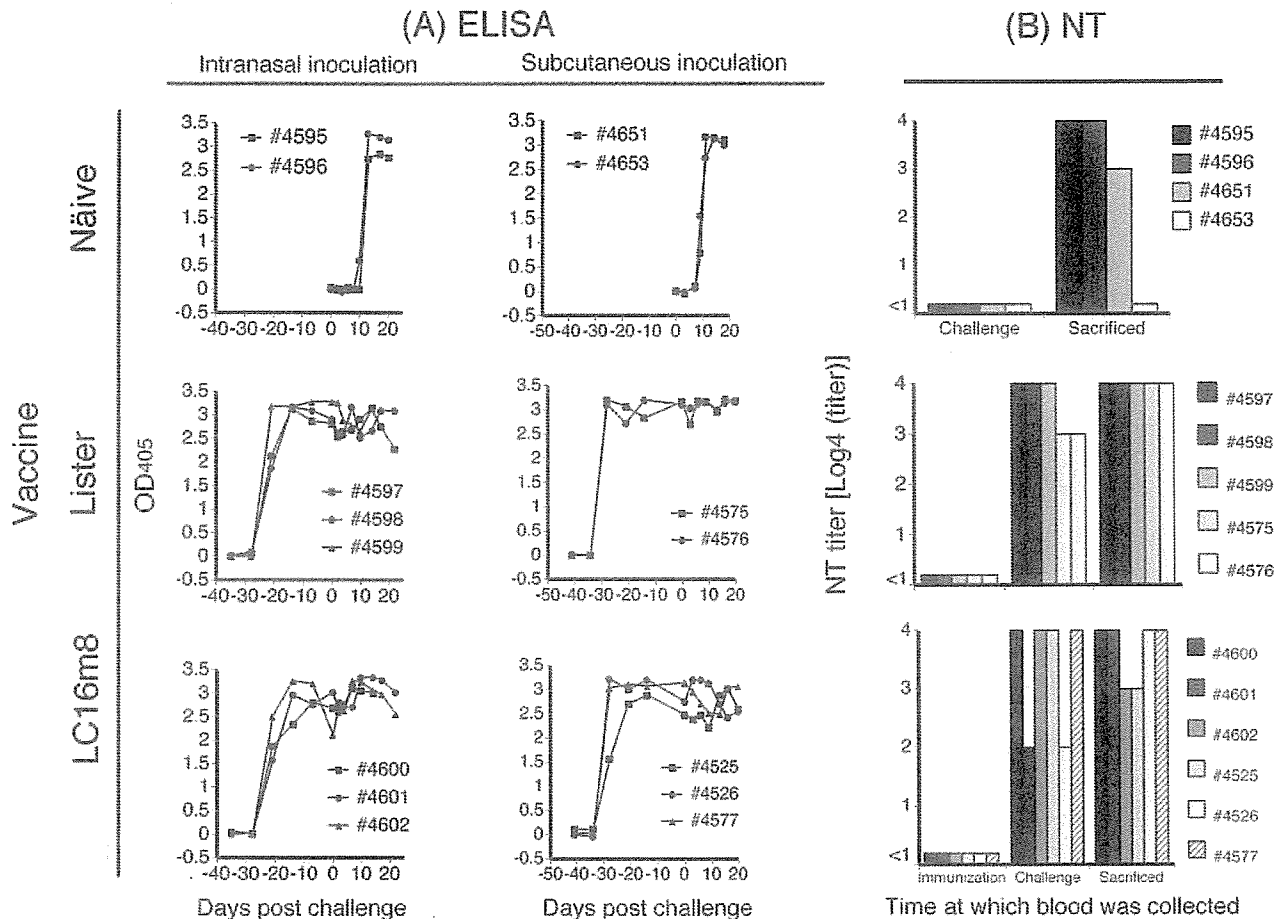
(A) ELISA   (B) NT

FIG. 5. Vaccinia virus-specific IgG responses determined by IgG ELISA (A) and a neutralizing assay (B) for MPXV. The optical densities at 405 nm (OD_{405}) at serum sample dilutions of 1:100 are shown. (A) Development of specific IgG antibody responses to vaccinia virus antigens in plasma samples collected on different days after vaccination and/or challenge, as measured by IgG ELISA. The day of MPXV challenge was taken as day zero. (B) MPXV-specific neutralizing antibody titers (NT) in plasma samples were determined by plaque reduction assay on different days after vaccination and/or challenge. The neutralizing antibody titers were determined for plasma collected from mice in the SC-Naïve group at the times of MPXV challenge and sacrifice and for plasma collected from mice in the SC-Lister and SC-LC16m8 groups at the times of immunization with Lister or LC16m8, challenge with MPXV, and sacrifice. The day of MPXV challenge was defined as day zero.

were examined. IFN-γ and IL-6 levels increased after MPXV challenge in groups IN-Naïve and SC-Naïve (Fig. 2). The levels of IFN-γ and IL-6 were higher in group SC-Naïve than in group IN-Naïve. The monkeys immunized with Lister or LC16m8 showed very low level or no detectable cytokine responses (Fig. 2).

Viremia determined by virus isolation and qPCR. Virus isolation results are summarized in Table 1. MPXV was isolated from purified PBMCs from group IN-Naïve between days 4 and 13 after challenge but not from PBMCs collected from any of the monkeys in groups IN-Lister and IN-LC16m8. MPXV was also isolated from the buffy coat fractions obtained from 4 ml of peripheral blood collected between days 3 and 14 from monkey 4651 and between days 3 and 18 from monkey 4653 in the SC-Naïve group. MPXV was isolated from the buffy coat fractions of two of the three SC-LC16m8 monkeys, but the plaque number was small and the isolation period was

short. MPXV was not isolated from any of the monkeys in the SC-Lister group.

The levels of viremia were assessed by qPCR with Light-Cycler using in-house primer sets and fluorescent probes. In the intranasal-inoculation model, viremia was demonstrated for group IN-Naïve but not for group IN-Lister or IN-LC16m8 (Fig. 2). In the subcutaneous-inoculation model, viremia was demonstrated for all monkeys in groups SC-Naïve and SC-LC16m8 and for one of the two monkeys in group SC-Lister. The levels and durations of viremia were highest and longest in group SC-Naïve, followed by group SC-LC16m8. These results were consistent with those of virus isolation experiments (Table 1 and Fig. 2).

IgG and neutralizing antibody responses. VV antigen-specific IgG became detectable by IgG-ELISA in monkeys immunized with Lister or LC16m8 within 2 weeks postimmunization (Fig. 5). The time courses and levels of IgG response deter-

mined by ELISA were similar for monkeys immunized with LC16m8 and those immunized with Lister (Fig. 5). IgG reactive to VV antigens became detectable by IgG-ELISA in the IN-Naïve and SC-Naïve groups within 2 weeks after MPXV challenge. The levels of neutralizing antibody to MPXV were tested before and after challenge with MPXV. At the time of challenge with MPXV, neutralizing antibody was detected in the monkeys immunized with LC16m8 or Lister. The titers were not increased after the challenge. Neutralizing antibody was demonstrated in both of the animals in the IN-Naïve group and in one of the two animals in the SC-Naïve group.

DISCUSSION

The protective efficacy of LC16m8 was evaluated in a mild-MPX nonhuman-primate model, in which monkeys were intranasally inoculated with MPXV strain Liberia, and in a lethal-MPX nonhuman-primate model, in which monkeys were subcutaneously inoculated with MPXV strain Zr-599. Monkeys subcutaneously inoculated with MPXV strain Liberia developed relatively milder symptoms of MPX than those subcutaneously inoculated with MPXV strain Zr-599. Monkeys intranasally inoculated with MPXV strain Liberia also developed relatively milder symptoms than those intranasally inoculated with MPXV strain Zr-599. These data suggest that MPXV strain Liberia, one of the West African strains, is less virulent than MPXV Zr-599, one of the Congo Basin strains (unpublished data).

A single vaccination with LC16m8 protected monkeys from MPX, as did a single vaccination with Lister. The results of the present study indicate that LC16m8 confers sufficient protection against MPX in monkeys, even in the lethal-MPX nonhuman-primate model. LC16m8 completely protected nonhuman primates from MPX in the intranasal-inoculation model. The protective efficacy of LC16m8 was confirmed not only with regard to clinical symptoms but also by virological assays, such as determination of the lymphocyte and thrombocyte counts, CRP level, and interleukin levels, viremia level determination by qPCR, virus isolation, and histopathological examinations. Differences between LC16m8 and Lister were observed only with respect to the viremia level and the cutaneous lesions at the site of virus inoculation after subcutaneous MPXV inoculation.

LC16m8 was reported to cause few adverse events when tested in a preliminary trial in which about 30,000 children were immunized in Japan in the 1970s (11). No serious complications were reported. Fever was observed in fewer cases than for Lister- or CV1-78-immunized individuals (11). The results of the present study strongly suggest that LC16m8 is as efficacious as Lister in protecting humans from smallpox or MPX and support the suggestion that LC16m8 may be useful as a replacement for currently available VVs, such as Lister and Dryvax. Especially, the risk of VV-related casualties must be minimized and avoided if VVs are used today, when there are no variola outbreaks. LC16m8 can also be used for the treatment of people in regions in which human MPX is endemic.

It has been reported that some of the characteristics of LC16m8, such as small-pock formation in chicken chorioallantoic membrane and a narrow host range for replication, are

due to a mutation in the membrane protein B5R (35). A single-nucleotide deletion in the *B5R* gene results in a deficiency in expression of full-length and intact B5R membrane protein (24, 35). There was a single-base deletion of G at the 274th position from the initiation codon, resulting in expression of a truncated B5R membrane protein. Although some poxvirus researchers have shown interest in the protective efficacy of LC16m8 (5), LC16m8 was shown to induce protective immunity to MPX in nonhuman primates in the present study. It was reported that the membrane protein B5R is not essential for protection against vaccinia virus infection in mice (19). Lister showed a stronger preventive effect against the local reactions at the site of MPXV inoculation in monkeys and resulted in lower levels of MPXV viremia than LC16m8. These observations suggest a role for the membrane protein B5R in induction of immunity to MPXV in nonhuman primates; however, the presence of the membrane protein B5R is not essential. Although the results of the present study cannot exclude the importance of the membrane protein B5R, LC16m8 induces sufficient protective immunity to MPX and probably induces protective immunity against variola.

Humans are usually infected with MPXV through the skin surface by bites from infected animals (9), while infection with variola occurs through the respiratory tract (7). In the present study, the monkeys were infected with MPXV by either the intranasal or the subcutaneous route in order to design an appropriate nonhuman-primate model not only for MPX but also for variola. The symptoms associated with MPX in naïve monkeys challenged intranasally with MPXV were somewhat milder than those reported in previous studies (15, 37, 39). This may have been due to the differences in MPXV strains, infection routes, or virus doses used for challenge. Subcutaneous infection of naïve monkeys with MPXV was fatal, but a single vaccination with LC16m8 prevented fatal infection. It must be emphasized that LC16m8 sufficiently protects monkeys even from lethal MPX.

In summary, a single vaccination with LC16m8 induced protective immunity against MPX, as did immunization with Lister, in nonhuman primates. These results strongly suggest that LC16m8 is also effective in the induction of high levels of protective immunity against variola.

REFERENCES

1. Cassimatis, D. C., J. E. Atwood, R. M. Engler, P. E. Linz, J. D. Grabenstein, and M. N. Vernalis. 2004. Smallpox vaccination and myopericarditis: a clinical review. J. Am. Coll. Cardiol. 43:1503–1510.
2. CDC. 2004. Update: adverse events following civilian smallpox vaccination—United States. 2003. Morb. Mortal. Wkly. Rep. 53:106–107.
3. Chen, N., G. Li, M. K. Liszewski, J. P. Atkinson, P. B. Jahrling, Z. Feng, J. Schriewer, C. Buck, C. Wang, E. J. Lefkowitz, J. J. Esposito, T. Harms, I. K. Damon, R. L. Roper, C. Upton, and R. M. Buller. 2005. Virulence differences between monkeypox virus isolates from West Africa and the Congo basin. Virology 340:46–63.
4. Chen, R. T., and J. M. Lane. 2003. Myocarditis: the unexpected return of smallpox vaccine adverse events. Lancet 362:1345–1346.

5. **Cohen, J.** 2002. Public health. Looking for vaccines that pack a wallop without the side effects. Science **298:**2314.

6. **Di Giulio, D. B., and P. B. Eckburg.** 2004. Human monkeypox: an emerging zoonosis. Lancet Infect. Dis. **4:**15–25.

7. **Esposito, J. J., and F. Fenner.** 2001. Poxviruses, p. 2887–2921. *In* D. M. Knipe, P. M. Howley, D. E. Griffin, R. A. Lamb, M. A. Martin, B. Roizman, and S. E. Straus (ed.), Fields virology, 4th ed., vol. 2. Lippincott Williams & Wilkins, Philadelphia, Pa.

8. **Galmiche, M. C., J. Goenaga, R. Wittek, and L. Rindisbacher.** 1999. Neutralizing and protective antibodies directed against vaccinia virus envelope antigens. Virology **254:**71–80.

9. **Guarner, J., B. J. Johnson, C. D. Paddock, W. J. Shieh, C. S. Goldsmith, M. G. Reynolds, I. K. Damon, R. L. Regnery, and S. R. Zaki.** 2004. Monkeypox transmission and pathogenesis in prairie dogs. Emerg. Infect. Dis. **10:**426–431.

10. **Halsell, J. S., J. R. Riddle, J. E. Atwood, P. Gardner, R. Shope, G. A. Poland, G. C. Gray, S. Ostroff, R. E. Eckart, D. R. Hospenthal, R. L. Gibson, J. D. Grabenstein, M. K. Arness, and D. N. Tornberg.** 2003. Myopericarditis following smallpox vaccination among vaccinia-naïve US military personnel. JAMA **289:**3283–3289.

11. **Hashizume, S., H. Yoshizawa, M. Morita, and K. Suzuki.** 1985. Properties of attenuated mutant of vaccinia virus, LC16m8, derived from Lister strain, p. 88–99. *In* G. V. Quinnan (ed.), Vaccinia viruses as vectors for vaccine antigens. Elsevier, Amsterdam, The Netherlands.

12. **Hatakeyama, S., K. Moriya, M. Saijo, Y. Morisawa, I. Kurane, K. Koike, S. Kimura, and S. Morikawa.** 2005. Persisting humoral antiviral immunity within the Japanese population after the discontinuation in 1976 of routine smallpox vaccinations. Clin. Diagn. Lab. Immunol. **12:**520–524.

13. **Hollinshead, M., G. Rodger, H. Van Eijl, M. Law, R. Hollinshead, D. J. Vaux, and G. L. Smith.** 2001. Vaccinia virus utilizes microtubules for movement to the cell surface. J. Cell Biol. **154:**389–402.

14. **Hooper, J. W., D. M. Custer, and E. Thompson.** 2003. Four-gene-combination DNA vaccine protects mice against a lethal vaccinia virus challenge and elicits appropriate antibody responses in nonhuman primates. Virology **306:**181–195.

15. **Hooper, J. W., E. Thompson, C. Wilhelmsen, M. Zimmerman, M. A. Ichou, S. E. Steffen, C. S. Schmaljohn, A. L. Schmaljohn, and P. B. Jahrling.** 2004. Smallpox DNA vaccine protects nonhuman primates against lethal monkeypox. J. Virol. **78:**4433–4443.

16. **Hu, G., M. J. Wang, M. J. Miller, G. N. Holland, D. A. Bruckner, R. Civen, L. A. Bornstein, L. Mascola, M. A. Lovett, B. J. Mondino, and D. A. Pegues.** 2004. Ocular vaccinia following exposure to a smallpox vaccinee. Am. J. Ophthalmol. **137:**554–556.

17. **Katz, E., B. M. Ward, A. S. Weisberg, and B. Moss.** 2003. Mutations in the vaccinia virus A33R and B5R envelope proteins that enhance release of extracellular virions and eliminate formation of actin-containing microvilli without preventing tyrosine phosphorylation of the A36R protein. J. Virol. **77:**12266–12275.

18. **Khodakevich, L., Z. Jezek, and D. Messinger.** 1988. Monkeypox virus: ecology and public health significance. Bull. W. H. O. **66:**747–752.

19. **Kidokoro, M., M. Tashiro, and H. Shida.** 2005. Genetically stable and fully effective smallpox vaccine strain constructed from highly attenuated vaccinia LC16m8. Proc. Natl. Acad. Sci. USA **102:**4152–4157.

20. **Kimura, M., and H. Sakai.** 1996. Complications of smallpox vaccination. Clin. Virol. **24:**30–39.

21. **Kitamura, T.** 1999. Smallpox eradication and future prospect of smallpox vaccine. Clin. Virol. **27:**378–384.

22. **Lane, J. M., and J. Goldstein.** 2003. Adverse events occurring after smallpox vaccination. Semin. Pediatr. Infect. Dis. **14:**189–195.

23. **Miller, J. R., N. M. Cirino, and E. F. Philbin.** 2003. Generalized vaccinia 2 days after smallpox revaccination. Emerg. Infect. Dis. **9:**1649–1650.

24. **Morikawa, S., T. Sakiyama, H. Hasegawa, M. Saijo, A. Maeda, I. Kurane, G. Maeno, J. Kimura, C. Hirama, T. Yoshida, Y. Asahi-Ozaki, T. Sata, T. Kurata, and A. Kojima.** 2005. An attenuated LC16m8 smallpox vaccine: analysis of full-genome sequence and induction of immune protection. J. Virol. **79:**11873–11891.

25. **Murphy, J. G., R. S. Wright, G. K. Bruce, L. M. Baddour, M. A. Farrell, W. D. Edwards, H. Kita, and L. T. Cooper.** 2003. Eosinophilic-lymphocytic myocarditis after smallpox vaccination. Lancet **362:**1378–1380.

26. **Nagata, N., T. Iwasaki, Y. Ami, A. Harashima, I. Hatano, Y. Suzaki, K. Yoshii, T. Yoshii, A. Nomoto, and T. Kurata.** 2001. Comparison of neuropathogenicity of poliovirus type 3 in transgenic mice bearing the poliovirus receptor gene and cynomolgus monkeys. Vaccine **19:**3201–3208.

27. **Nagata, N., H. Shimizu, Y. Ami, Y. Tano, A. Harashima, Y. Suzaki, Y. Sato, T. Miyamura, T. Sata, and T. Iwasaki.** 2002. Pyramidal and extrapyramidal involvement in experimental infection of cynomolgus monkeys with enterovirus 71. J. Med. Virol. **67:**207–216.

28. **Neubauer, H., U. Reischl, S. Ropp, J. J. Esposito, H. Wolf, and H. Meyer.** 1998. Specific detection of monkeypox virus by polymerase chain reaction. J. Virol. Methods **74:**201–207.

29. **Newsome, T. P., N. Scaplehorn, and M. Way.** 2004. SRC mediates a switch from microtubule- to actin-based motility of vaccinia virus. Science **306:**124–129.

30. **Reed, K. D., J. W. Melski, M. B. Graham, R. L. Regnery, M. J. Sotir, M. V. Wegner, J. J. Kazmierczak, E. J. Stratman, Y. Li, J. A. Fairley, G. R. Swain, V. A. Olson, E. K. Sargent, S. C. Kehl, M. A. Frace, R. Kline, S. L. Foldy, J. P. Davis, and I. K. Damon.** 2004. The detection of monkeypox in humans in the Western Hemisphere. N. Engl. J. Med. **350:**342–350.

31. **Saurina, G., S. Shirazi, J. M. Lane, B. Daniel, and L. DiEugenia.** 2003. Myocarditis after smallpox vaccination: a case report. Clin. Infect. Dis. **37:**145–146.

32. **Schmelz, M., B. Sodeik, M. Ericsson, E. J. Wolffe, H. Shida, G. Hiller, and G. Griffiths.** 1994. Assembly of vaccinia virus: the second wrapping cisterna is derived from the trans Golgi network. J. Virol. **68:**130–147.

33. **Semba, R. D.** 2003. The ocular complications of smallpox and smallpox immunization. Arch. Ophthalmol. **121:**715–719.

34. **Smith, G. L., A. Vanderplasschen, and M. Law.** 2002. The formation and function of extracellular enveloped vaccinia virus. J. Gen. Virol. **83:**2915–2931.

35. **Takahashi-Nishimaki, F., S. Funahashi, K. Miki, S. Hashizume, and M. Sugimoto.** 1991. Regulation of plaque size and host range by a vaccinia virus gene related to complement system proteins. Virology **181:**158–164.

36. **Takahashi-Nishimaki, F., K. Suzuki, M. Morita, T. Maruyama, K. Miki, S. Hashizume, and M. Sugimoto.** 1987. Genetic analysis of vaccinia virus Lister strain and its attenuated mutant LC16m8: production of intermediate variants by homologous recombination. J. Gen. Virol. **68:**2705–2710.

37. **Weltzin, R., J. Liu, K. V. Pugachev, G. A. Myers, B. Coughlin, P. S. Blum, R. Nichols, C. Johnson, J. Cruz, J. S. Kennedy, F. A. Ennis, and T. P. Monath.** 2003. Clonal vaccinia virus grown in cell culture as a new smallpox vaccine. Nat. Med. **9:**1125–1130.

38. **Whitman, T. J., M. A. Ferguson, and C. F. Decker.** 2003. Cardiac dysrhythmia following smallpox vaccination. Clin. Infect. Dis. **37:**1579–1580.

39. **Zaucha, G. M., P. B. Jahrling, T. W. Geisbert, J. R. Swearengen, and L. Hensley.** 2001. The pathology of experimental aerosolized monkeypox virus infection in cynomolgus monkeys (*Macaca fascicularis*). Lab. Investig. **81:**1581–1600.

Original article

Tristetraprolin inhibits HIV-1 production by binding to genomic RNA

Masae Maeda [a,b,c], Hirofumi Sawa [c,d,e], Minoru Tobiume [a], Kenzo Tokunaga [a], Hideki Hasegawa [a], Takeshi Ichinohe [a], Tetsutaro Sata [a], Masami Moriyama [b], William W. Hall [f], Takeshi Kurata [a], Hidehiro Takahashi [a,*]

[a] Department of Pathology, National Institute of Infectious Diseases, Toyama 1-23-1, Shinjuku-ku, Tokyo 162-8640, Japan
[b] Department of Microbiology and Immunology, School of Medicine, Keio University, Tokyo, Japan
[c] CREST, JST, Japan
[d] Department of Molecular Pathobiology, Hokkaido University Research Center for Zoonosis Control, Hokkaido University, Sapporo, Japan
[e] 21st Century COE Program for Zoonosis, Hokkaido University, Sapporo, Japan
[f] Department of Medical Microbiology, Conway Institute of Biomolecular and Biomedical Research, University College Dublin, Belfield, Dublin, Ireland

Abstract

HIV-1 genome has an AU-rich sequence and requires rapid nuclear export by Rev activity to prevent multiple splicing. HIV-1 infection occurs in activated CD4+ T cells where the decay of mRNAs of cytokines and chemokines is regulated by the binding of AU-rich elements to the mRNA-destabilizing protein tristetraprolin. We here investigated the influence of tristetraprolin on the replication of HIV-1. Treatment of siRNA against tristetraprolin in a latently HIV-1 infected cell line increases HIV-1 production following stimulation. A chloramphenicol acetyltransferase and luciferase assay revealed that exogenous tristetraprolin reduced HIV-1 virion production and in contrast increased the multiply spliced products. Furthermore, quantitative RT–PCR analysis showed tristetraprolin increases the ratio of multiple-spliced RNAs to un-, single-spliced RNA. Moreover, an electrophoretic mobility shift assay showed that tristetraprolin binds to synthesized HIV-1 RNA with AU-rich sequence but not to RNA with less AU sequence. These results suggest that tristetraprolin is a regulator of HIV-1 replication and enhances splicing by direct binding to AU-rich sequence of HIV-1 RNAs.
© 2006 Elsevier Masson SAS. All rights reserved.

Keywords: Human immunodeficiency virus type 1; Tristetraprolin; AU-rich element

1. Introduction

Expression of human immunodeficiency virus type 1 (HIV-1) genes is regulated by several posttranscriptional mechanisms,

which include RNA splicing, stability, transport and translation. For example, HIV-1 RNA contains inhibitory sequences (INS) negatively regulating expression [1], which is also known to be AU-rich [2]. Replacement of AU residues of HIV-1 mRNA has been reported to result in a marked increase in expression of HIV-1 Gag, Pol, and Env proteins independent of the Crm1/Rev/Rev-responsive element (RRE) export pathway [3]. In addition, another nuclear export system, constitutive transport elements (CTE)/Tap, can substitute Rev/RRE [4], suggesting that effective nuclear export is required to complement the character of AU-rich RNA genome. As we have previously reported that HIV-1 RNA is fragmented

in viral particles and in vitro-synthesized HIV-1 RNA is cleaved between U and A or C and A [5], effective nuclear export of HIV-1 RNA by Crm1/Rev/RRE might be required to rescue a potentially unstable RNA genome, and the balance between RNA decay and nuclear export could be an important facet of HIV-1 replication and pathogenesis.

Whereas activated CD4$^+$ T cells are a primary target for productive HIV-1 infection [6], HIV-1 production does not occur in resting CD4$^+$ T cells because of a low level of reverse transcriptase activity [7]. In activated cells, including CD4$^+$ T cells that produce cytokines, chemokines and other proteins in response to inflammation and infection, mRNAs are degraded rapidly following transient activation [8]. These mRNAs contain the AU-rich element (ARE) in their 3′-untranslated region (3′UTR) that binds with tristetraprolin (TTP, also known as TIS11, Nup475, or G0S24) [9]. TTP is the prototype of a family of proteins that possess a pair of closely spaced zinc fingers of the CCCH class and are capable to binding AU-rich elements (ARE) in the 3′UTR and subsequent destruction of transcripts of pro-inflammatory mediators such as tumor necrosis factor α, granulocyte/macrophage colony stimulating factor, and cyclooxygenase 2 [10].

We propose the hypothesis that TTP might interact with the AU-rich regions of HIV-1 RNA and that the regulation of the HIV-1 RNA genome could play important roles in the post-transcriptional control of HIV-1 replication in activated or memory T cells. We show that TTP reduced HIV-1 virion production by enhancing multiple splicing through binding to HIV-1 AU-rich RNA.

2. Materials and methods

2.1. Cell culture

The human cell lines HEK293T and HeLa were maintained under an atmosphere of 5% CO_2 at 37 °C in Dulbecco's modified Eagle's medium supplemented with 10% fetal bovine serum. U1 cells [11] were cultured in complete medium (RPMI 1640 medium supplemented with 10% fetal bovine serum).

2.2. RNAi inhibition

siRNA treatment was achieved using synthetic oligonucleotides which were purchased from Ambion. Sense sequence of TTP siRNA is CCC AUA AAU CAA UGG GCC Ctt (small capital displays deoxyribonucleic acid) and antisense is GGG CCC AUU GAU UUA UGG Gtg. Two rounds of siRNA treatments were performed. siRNA was transfected by using the electric transfection apparatus, amaxa in U1 cells.

2.3. Cloning, mutagenesis, and plasmid construction for TTP or rev expression vectors

Polyadenylated RNA was isolated from HeLa cells and subjected to reverse transcription (RT) with SuperScript RNaseH$^-$ reverse transcriptase (Invitrogen Life Technologies) and a 15-nucleotide poly(dT) primer. The coding region of human TTP cDNA was amplified by polymerase chain reaction (PCR) with the reverse-transcribed cDNA as the template and with the primers 5′-CGT GAATTC ATG GAT CTG ACT GCC ATC TAC GAG AGC CT-3′ (TTPF, *Eco*RI site underlined) and 5′-GAC CGG GCA G GCGGCCGC TCA CTC AGA AAC AGA GAT-3′ (TTPR, *Not*I site underlined). The PCR product was digested with *Eco*RI and *Not*I and then cloned into pcDNA4/HisMax-C (Invitrogen Life Technologies), a mammalian expression vector containing the Xpress epitope tag sequence, or into pCAGGS-IRES-EGFP [12], yielding pchTTPwt or pCAGGSTTP, respectively. The resulting plasmids were sequenced with a DNA sequencer (model 377A; Perkin Elmer, Norwalk, CT). Expression vectors for TTP deletion mutants, including 1—101, 76—189, and 176—320, were similarly constructed with pchTTPwt as the template and with the primers 5′-TCT CTG AG GCGGCCGC TTA TAG CTC AGT CTT GTA GCG CGA -3′ (R1—101), 5′-CTG GCT GAATTC CTG GGC CCT GAG CTG TCA CCCT-3′ (F76—189), 5′-AGG CCT GGT GCGGCCGC TTA GGT CCG GCG GCC AGA GGG CA-3′ (R76—189), and 5′-CCT GTG GAATTC CAG AGC ATC AGC TTC TCC GGC CT-3′ (F176—320). The resulting expression vectors were designated pcD1—101, pcD76—189, and pcD176—320, respectively.

For construction of vectors for Xpress-tagged Rev, the Rev cDNA was amplified by PCR with pSRαRev [13] as the template and with the primers 5′-AAA AAA AGATCT ATG GCA GGA AGA-3′ (Rev-*Bgl*II) and 5′-AAA AAAGTCGAC CTA TTC TTT AGTT-3′ (Rev-*Sal*I). The PCR product was digested with *Bgl*II and *Sal*I and then cloned into pEGFP-C1 (BD Biosciences Clontech, Palo Alto, CA) or pcDNA4/HisMax-C that had been digested with *Bam*HI and *Xho*I; the resulting vectors were designated pEGFP-Rev or pcMax-Rev.

2.4. Luciferase, chloramphenicol acetyltransferase (CAT), and p24 enzyme-linked immunosorbent (ELISA) assays

HEK293T cells were cotransfected with HIV-1 proviral DNA (pNL43 [14], pNL-Luc-E$^-$R$^+$ [15], or pNL-enCAT [16]) and TTP expression vectors (pchTTPwt, pcD1—101, pcD76—189, or pcD176—320) with the use of Fugene 6 (Roche, Mannheim, Germany) or by the calcium phosphate method. The amount of virus in culture supernatants was quantified by measurement of p24 antigen with a p24 Gag antigen capture ELISA assay (ZeptoMetrix, Buffalo, NY). For measurement of luciferase activity or CAT [17], cells were lysed and assayed with a Luciferase Assay System (Promega, Madison, WI) and a Lumat LB 96V luminometer (Perkin Elmer) or with a CAT ELISA (Roche).

Expression of wild-type and mutant TTP was examined by immunoprecipitation, SDS—polyacrylamide gel electrophoresis and immunoblot with mouse monoclonal antibodies to the Xpress epitope (Invitrogen) analysis or goat polyclonal antibodies to TTP (Santa Cruz Biotechnology, Santa Cruz, CA). The antibodies to Nef and to p24 also used for immunoblot analysis were kind gifts from Dr. Ikuta. Signals were obtained

with the ECL detection system (Amersham Pharmacia) and digitized with an LAS1000 imaging system (Fujifilm, Tokyo, Japan).

2.5. RT—PCR and virus infection

Cellular total RNA or virion RNA was subjected to RT with a 15-nucleotide poly(dT) primer and the use of an Omniscript kit (Qiagen, Valencia, CA). The resulting cDNA was subjected to quantitative analysis with a real-time, 5′-exonuclease PCR-based assay (TaqMan) and primer—probe combinations that were selected with the use of Primer Express software (Applied Biosystems, Foster City, CA) as specific for the coding regions of the tat, env, or luciferase genes. The reaction was performed with a QuantiTect Probe PCR kit (Qiagen) and an amplification protocol comprising incubation at 95 °C for 15 min followed by 45 cycles of 95 °C for 15 s and 60 °C for 1 min. The primers 1459F (5′-GGT CCT ATG ATT ATG TCC GGT TATG-3′) and 1535R (5′-TGT AGC CAT CCA TCC TTG TCAA-3′), and the probe 1491P (5′-FAM-TCC GGA AGC GAC CAA CGC CTT-TAMRA-3′, in which FAM indicates 6-carboxyfluorescein and TAMRA indicates N,N,N',N'-tetramethyl-6-carboxyrhodamine) were used for detection of luciferase cDNA; the primers 7484F (5′-ATA AAC ATG TGG CAG GAA GTA GGAA-3′) and 7572R (5′-AGC AGC CCA GTA ATA TTT GAT GAAC-3′), and the probe 7513P (5′-FAM-AAT GTA TGC CCC TCC CAT CAG TGG ACA-TAMRA-3′) were used for that of env cDNA; the primers 6016F (5′-CAG ACT CAT CAA GCT TCT CTA TCA AAG-3′) and 8465R (5′-CGT TCA CTA ATC GAA TGG ATC TGT-3′), and the probe 8392P (5′-FAM-ACC CGA CAG GCC CGA AGG AAT AGA A-TAMRA-3′) were used for that of rev, tat and nef cDNA; the primers 5918F (5′-GTT GCT TTC ATT GCC AAG TTTG-3′) and 6017R (5′-TGA CTG TTC TGA TGA GCT CTT CGT-3′), and the probe 5945P (5′-FAM-TGA CA A AAG CCT TAG GCA TCT CCT ATG GC-TAMRA-3′) were used for that of the second exon of tat; the primers TTP 405F (5′-GCT GCG CCA GGC CAA TC-3′) and TTP 477R (5′-GCA GCG GCC CTG GAG GTA-3′), and the probe TTP 423 (5′-FAM- CCA CCC CAA ATA CAA GAC GGA ACT CTG TC-3′) were used for that of TTP cDNA. The transcripts detected by the env region primers and probe include both unspliced (9 kb) and singly-spliced (4 kb) RNA molecules, whereas those detected by the tat, rev and nef cDNA primers and probe include multiply-spliced transcripts (2 kb) [15]. The RNA copy numbers of luciferase, HIV-1 transcripts and TTP were determined with pGL3-promoter, pNL-Luc-E⁻R⁺, pSRαRev and pchTTPwt as a standard, respectively.

Vesicular stomatitis virus envelope-glycoprotein (VSV-G)-pseudotyped HIV-1 was produced by cotransfection of pNL-Luc-E⁻R⁺ and the VSV-G expression vector pHIT/G [18] in HEK293T cells. VSV-G-pseudotyped NL-Luc virus was infected to HEK293T cells transfected with TTP-expression vector or an empty vector. Following exposure to actinomycin D, an inhibitor of transcription, the copy numbers of multiple
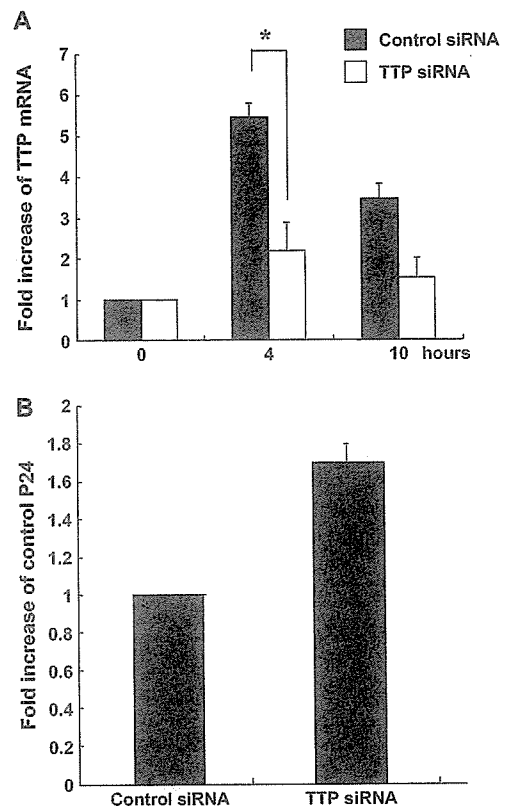

Fig. 1. Reduction of endogenous TTP increased HIV-1 production in U1 cells. (A) U1 cells were treated with two rounds of siRNA for TTP and controls. Following exposure to 7.5 ng/ml of PMA for 0, 4, or 10 h, the amount of TTP mRNAs were determined by RT—PCR and represented as the relative ratio against that of the cells before exposure to PMA. Data are means ± S.D. of values from three independent experiments. (B) Viral products (p24) of the supernatants of similarly treated cells as in (A) after 48 h post PMA stimulation were measured. *$P < 0.05$.

spliced or un-, singly spliced transcripts were determined by RT—PCR.

2.6. Preparation of RNA substrates

Substrate RNAs were prepared by in vitro transcription with T7 RNA polymerase and DNA amplified by the PCR as the template. DNA fragments that include the T7 promoter and encode RNA substrates of 75 and 93 nucleotides (nt) corresponding to the p7 and RRE were thus synthesized by PCR with the following primers: p7F (5′-TAA TAC GAC TCA CTA TAG GGA ACA AAT CCA GCT ACC ATA ATG ATA-3′) (underlining denotes T7 promoter) and P7R (5′-ATT GAA ACA CTT AAC AGT CTT-3′), corresponding to nt 1900 to 1971 of pNL43, GenBank accession number, M19921; stem II of RRE; U-GF (5′- AAA TAA TAC GAC TCA CTA TA GGGAG CAG CAG GAA GCA CTA TGG GCT-3′) and U-GR (5′-TTG TTC TGC TGC TGC ACT ATA TCA GAC AAT-3′), corresponding to nt 7783 to 7875. The RNA molecules were labeled at the 5′ end with [γ-³²P]ATP and

polynucleotide kinase after dephosphorylation with calf intestinal phosphatase. They were purified by electrophoresis on denaturing 15% polyacrylamide gels containing 7 M urea with the use of a Mini Whole Gel Eluter (Bio-Rad, Hercules, CA). The concentration of RNAs was determined by spectrophotometer (NanoDrop technology, Wilmington, DE).

2.7. Analysis of proteins and enzyme purification

Recombinant TTP protein was produced by overexpression in Escherichia coli using an His$_6$-tagged prokaryotic expression vector, pQE-9 (Qiagen) encoding TTP cDNA (GenBank accession number, M63625) [19]. Recombinant proteins were purified using an HiTrap chelating column (Amersham Pharmacia, Biotech, Freiburg, Germany) [20]. After staining with SYPRO (Molecular Probes), the polyacrylamide gel was visualized with FLA 2000 (Fujifilm).

2.8. Immunofluorescence analysis

HeLa cells were transfected with pEGFP-Rev and either pcDNA4/HisMax-C, pchTTPwt, pcD1–101, pcD76–189, or pcD176–320. After 24 h, the transfection mixture was removed and the cells were washed twice with phosphate-buffered saline (PBS), treated with 0.5% trypsin in 0.1 mM EDTA, suspended in culture medium, and plated on coverslips. The cells were then incubated for 2 h at 37 °C, fixed for 1 h at room temperature with 4% paraformaldehyde in PBS, and permeabilized for 5 min with 0.1% Triton X-100 in PBS. After quenching with 0.1 M NH$_4$Cl at room temperature for 10 min, the cells were incubated with 10% fetal bovine serum in PBS before consecutive exposures for 1 h at room temperature first to antibodies to the Xpress epitope in PBS containing 0.5% gelatin, 10 mM glycine, 10 mM EDTA, and 0.05% NaN$_3$ and then to Alexa Fluor 543-conjugated goat polyclonal antibodies to mouse immunoglobulin
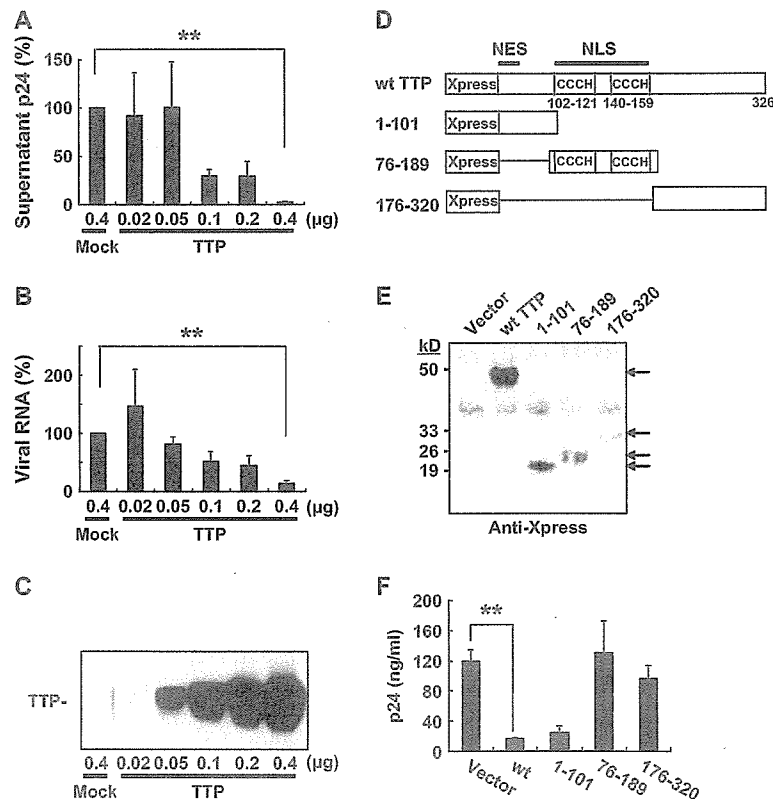

Fig. 2. Suppression of HIV-1 production by exogenous TTP. HEK293T cells (5 × 10^5 per well in a 12-well dish) were cotransfected with HIV-1 proviral DNA (0.04 μg of pNL-Luc-E R$^+$) and either the indicated amounts of an expression vector for TTP tagged with the Xpress epitope (pchTTPwt) or the corresponding empty vector (0.4 μg). The cells were subsequently cultured for 48 h in fresh medium, after which the amounts of p24 (A) and HIV-1 genomic RNA (the second exon of tat) (B) in the culture supernatants were determined; data are expressed as a percentage of the values for cells transfected with the empty expression vector and are means ± S.D. of values from three independent experiments. Cell lysates were also subjected to immunoblot analysis with an antibody to the Xpress epitope tag (C). **$P < 0.02$. (D) Schematic representation of TTP mutants. Xpress tag, zinc finger domain (CCCH), nuclear export signal (NES), nuclear localization sequence (NLS) and the number of amino acid (326) are indicated. (E) Immunoprecipitation using an antibody to the Xpress epitope of the lysates from HEK293T cells expressing Xpress-tagged wild-type (wt) or mutant forms of TTP, followed by immunoblot analysis with the same antibody. (F) HEK293T cells (5 × 10^5) were cotransfected with pNL-Luc-E R$^+$ (0.04 μg) and either an expression vector for wild-type or mutant TTP (0.4 μg) or the corresponding empty vector. The cells were subsequently cultured for 48 h in fresh medium, after which the amount of p24 in the culture supernatants was determined. Data are means ± S.D. of values from three independent experiments. **$P < 0.02$.